Reviewed Preprint
v1 • November 13, 2025
Not revised

Reviewed Preprint
v2 • March 5, 2026
Revised by authors

Hugin-AstA circuitry is a novel central energy sensor that directly regulates sweet sensation in *Drosophila* and mouse

Wusa Qin[1,*], Tingting Song[2,3,*], Zeliang Lai[4], Daihan Li[3], Liming Wang[1,2,3] ✉, Rui Huang[3,5] ✉

[1]Institute of Molecular Physiology, Shenzhen Bay Laboratory, Shenzhen, China • [2]School of Public Health, Capital Medical University, Beijing, China • [3]Chinese Institutes for Medical Research, Beijing, China • [4]Center for Neurointelligence, School of Medicine, Chongqing University, Chongqing, China • [5]Guangyang Bay Laboratory, Chongqing Institute for Brain and Intelligence, Chongqing, 400060, China

For correspondence:
lmwang83@ccmu.edu.cn
huangrui0716@sina.com

* These authors contribute equally to this work.

Competing interests: No competing interests declared

Funding: See page 30

Reviewing editor: Meet Zandawala, University of Nevada, Reno, United States

eLife Assessment

This **important** work by Qin et al. delineates layered neuropeptidergic mechanisms that regulate sugar intake in a hunger state-dependent manner. Using a combination of genetic, physiological, and behavioral experiments, the authors **convincingly** show that Hugin- and Allatostatin A-releasing neurons are selectively active in sated flies and suppress sugar feeding by reducing the sensitivity of Gr5a-expressing gustatory neurons. They further demonstrate that Neuromedin U neurons share key physiological properties with fly Hugin neurons, highlighting conserved peptide functions across animal phyla.

https://doi.org/10.7554/eLife.108551.2.sa3

Abstract

Taste sensation plays a crucial role in shaping feeding behavior and is intricately influenced by internal states like hunger or satiety. Despite the identification of numerous neural substrates regulating feeding behavior, the central neural substrate that linked energy-sensing and taste sensation remained elusive. Here, we identified a novel neural circuitry that could directly sense internal energy state and modulate sweet sensation in the Drosophila brain. Specifically, a subset of neuropeptidergic neurons expressing hugin directly detected elevated levels of circulating glucose via glucose transporter Glut1 and ATP-sensitive potassium channel. Upon activation, these neurons released hugin peptide and activated downstream Allatostatin A (AstA)$^+$ neurons via its cognate receptor PK2-R1. Subsequently, the activation of AstA$^+$ neurons then directly inhibited sweet sensation via AstA peptide and its cognate receptor AstA-R1 expressed in sweet-sensing Gr5a$^+$ neurons. We also showed that neuromedin U (NMU), the mammalian homolog of fly hugin, served as an energy sensor to suppress sweet sensation. Therefore, these data identify hugin$^+$ neuron as a central energy sensor responsible for regulating sweet sensation across species.

Introduction

Animal behavior is tightly coupled to internal metabolic states[1]. Hunger profoundly alters feeding-related behaviors, enhancing sensitivity to appetitive cues and promoting food-seeking, whereas satiety actively suppresses these responses to shift behavioral priorities[2,3]. Such state-dependent modulation allows animals to dynamically allocate resources to maintain energy homeostasis[4]. While the neural mechanisms that drive feeding during hunger have been extensively characterized[5], the central circuits that sense satiety signals—specifically circulating glucose—to directly inhibit sensory processing remain less understood.

In both mammals and insects, "hunger signals" act as powerful accelerators for feeding. In the mammalian hypothalamus, AgRP neurons are activated by energy deficits to promote consumption[6,7], while in *Drosophila*, dopaminergic and Neuropeptide F (NPF) pathways increase the gain of sweet-sensing gustatory neurons to drive sugar intake[8–10]. These systems explain how animals ramp up feeding motivation when energy is low. However, to prevent overconsumption, the brain must also possess precise "braking" mechanisms that detect elevated energy states and rapidly dampen sensory sensitivity.

Dietary sugar is a primary satiety signal[11], yet the pathway linking central sugar sensing to behavioral inhibition remains elusive. In *Drosophila*, high-sugar diets are known to reduce sweet sensation via gut-derived signals or through central sensors like insulin-producing cells and DH44-expressing neurons that regulate general metabolic states[12–14]. Despite these advances, a critical gap remains: identifying a direct central sensor that detects acute rises in circulating glucose and acts specifically to inhibit the peripheral sweet-sensing machinery. Hugin-expressing neurons are promising candidates for this role, as they have been implicated in satiety-related feeding regulation[15,16]. Furthermore, Allatostatin A (AstA) has been proposed as a downstream signal capable of inhibiting sweet sensation[17]. However, whether and how these components form a unified circuit to sense glucose and apply the "brake" on feeding has not been established.

Here, we identify a complete neural circuitry that bridges this gap, directly linking internal glucose levels to the modulation of sweet taste sensation. We show that a specific subpopulation of hugin-expressing neurons functions as a central energy sensor, detecting elevated circulating glucose via the glucose transporter Glut1 and ATP-sensitive potassium channels. Upon activation, these neurons release hugin neuropeptide to activate downstream AstA-expressing neurons via the PK2-R1 receptor. Subsequently, AstA neurons directly inhibit sweet-sensing Gr5a$^+$ gustatory neurons through AstA–AstA-R1 signaling. This pathway functions as a dedicated satiety-dependent brake, suppressing sweet sensitivity in fed flies. Finally, we demonstrate that Neuromedin U (NMU), the mammalian homolog of hugin[18], similarly acts as a central energy sensor in mice to modulate sweet-responsive circuits, revealing a conserved neural strategy for coupling metabolic state to sensory processing across species.

Results

hugin$^+$ neurons were a novel glucose sensor in the fly brain

Flies extend their proboscis in response to appetitive cues, a behavioral element known as the proboscis extension reflex (PER) [20,51]. As previously observed, hunger significantly enhances this reflex[20]. In our study, we first replicated this phenomenon: In the state of hunger, flies exhibited elevated PER towards various concentrations of sugar compared to those under fed conditions (Figure 1A-B). These results confirmed the notion that sweet sensation was influenced by the internal energy state, elevated by starvation and suppressed by satiety [20,52]. Sweet sensation in flies is mediated by sweet-sensing Gr5a$^+$ neurons located on the proboscis [53]. Consistent with the behavioral effect, we also confirmed that Gr5a$^+$ neurons exhibited elevated calcium responses to sugar under starvation conditions (Figure supplementary 1A).

Dopaminergic neurons in the subesophageal zone (SEZ) region of the fly brain acted as a hunger sensor, promoting sweet sensation via a specific dopamine receptor DopEcR expressed in Gr5a$^+$ neurons [20,52]. However, although the gene knockout of tyrosine hydroxylase (TH) [54], a key enzyme for dopamine biosynthesis, significantly suppressed sweet sensation in starved fruit flies (Figure supplementary 1B), these flies still showed a further reduction in sugar-induced PER under sated conditions (Figure supplementary 1C-D). These results suggest the existence of dopamine-independent mechanisms for sensing satiety and hunger in fruit flies that exerts modulatory effect on sweet sensation.

In the terminating phase of feeding behavior, satiety signals play a crucial role to cease food consumption and to ensure an appropriate amount of food ingestion. A number of neuropeptidergic neurons were identified as putative satiety signals [36]. Notably, some of these neurons, including those secreting neuropeptides LK, TK, hugin, AstA, CCHa1, and CCHa2, are also

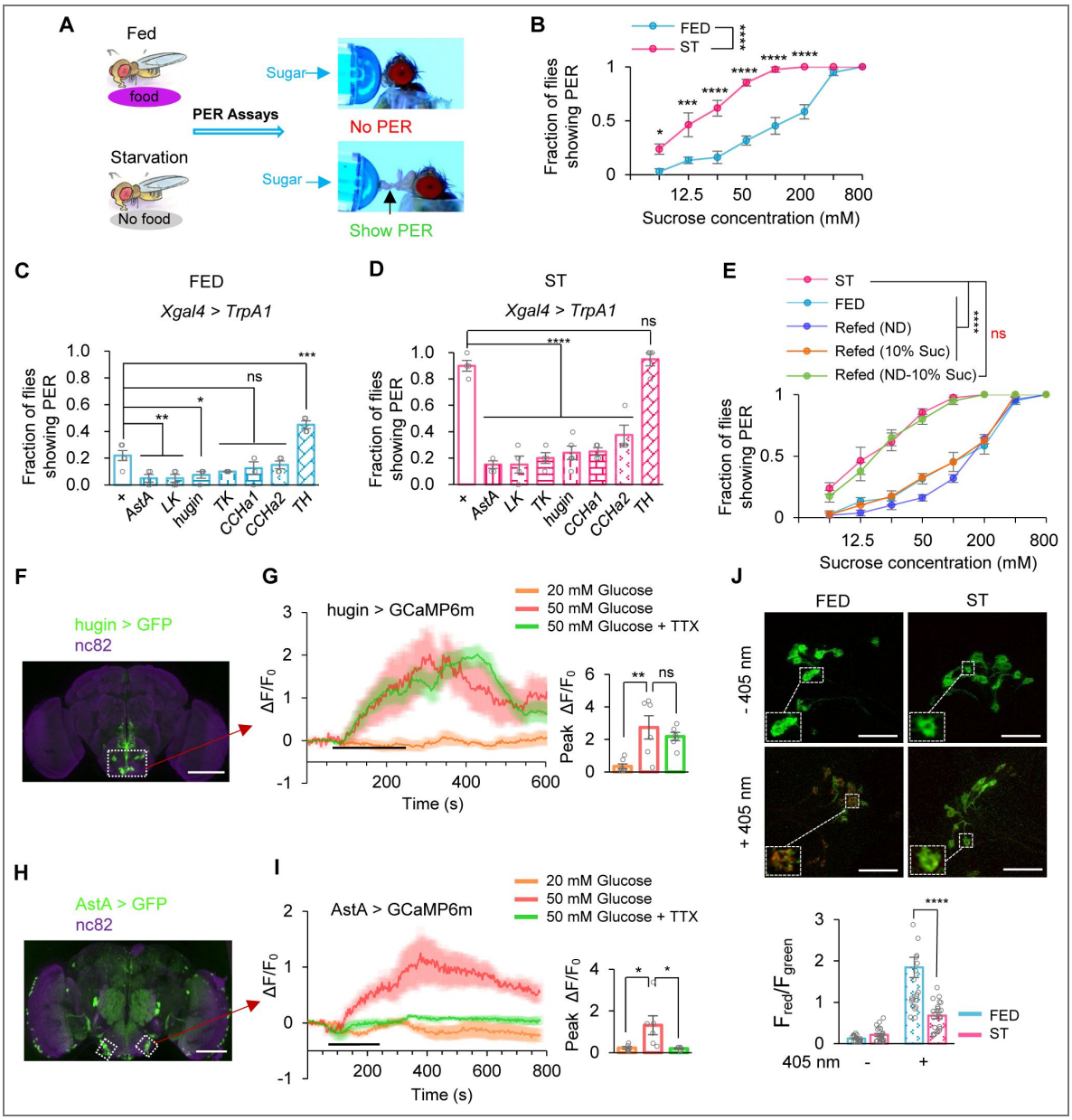

Figure 1. hugin^{+} neurons were a novel glucose sensor in the fly brain.

(**A**) Experimental procedure schematic. Newly eclosed flies were gathered and provided with regular food for 5 days, followed by a 12-hour period of starvation. Proboscis Extension Response (PER) assays were conducted. (**B**) Fraction of flies showing PER to different concentrations of sucrose (n=4 groups, each of 10 flies). (**C-D**) Fraction of flies of the indicated genotypes under 30 °C showing PER to 400 mM of sucrose (n=4-5 groups, each of 10 flies). (**E**) Fraction of indicated flies showing PER to different concentrations of sucrose (ND represent standard fly food) (n=4-5 groups, each of 10 flies). (**F**) hugin expression in the brain, illustrated by mCD8::GFP expression driven by *hugin^{GAL4}*. Scale bar represents 100 μm. (**G**) Representative traces and quantification of ex vivo calcium responses of hugin^{+} neurons during the perfusion of glucose with or without TTX (n=6-7). Horizontal black bar represents the duration indicated glucose solution stimulation. (**H**) AstA expression in the brain, illustrated by mCD8::GFP expression driven by *AstA^{GAL4}*. Scale bar represents 100 μm. (**I**) Representative traces and quantification of ex vivo calcium responses of AstA^{+} neurons during the perfusion of glucose with or without TTX (n=6). (**J**) Representative images of pre-photoconversion (pre-PC) and post-photoconversion (post-PC) CaMPARI signal in hugin-expressing neurons (upper). The Red:Green ratio represents intracellular Ca^{2+} concentrations (lower). Scale bar represents 100 μm (n=18-23). ns, P > 0.05; *P < 0.05; **P < 0.01; ***P < 0.001; ****P < 0.0001. Student's *t-test*, one-way and two-way ANOVA followed by post hoc test with Bonferroni correction were used for multiple comparisons when applicable.

distributed in the SEZ region [55]. It has been reported that the sweet-sensing gustatory neurons primarily receive regulatory inputs from neurons in the SEZ region [20,51]. Therefore, we hypothesized that these neuropeptidergic neurons might function as satiety signals, imposing inhibititory effect on sweet sensation after adequate food ingestion.

To test this hypothesis, we selectively expressed the temperature-sensitive ion channel TrpA1 in these neurons and activated them at 30 °C, triggering the release of corresponding neuropeptides. Indeed, activation of LK-, TK-, hugin-, AstA-, CCHa1-, and CCHa2-expressing neurons robustly suppressed sweet taste sensitivity in both fed and starved flies (Figure 1C–D; ***also see*** Figure supplementary 2). Moreover, LK-, TK-, and hugin-expressing neurons exerted particularly strong inhibition under satiated conditions (Figure 1C–D***; also see*** Figure supplementary 2). These results reveal a multilayered, state-dependent neuropeptidergic network that finely tunes gustatory processing and feeding behavior. In contrast, activating dopaminergic neurons enhanced sweet perception in sated flies as expected (Figure 1C). In starved flies, activating dopaminergic neurons elicited no change in PER likely due to a ceiling effect (Figure 1D).

In mammals and flies, circulating sugar levels are directly linked to satiety/hunger state [11,36,56]. We then asked whether changes in circulating sugar levels exerted an effect on sweet sensation. Activating IPCs in the fly brain released *Drosophila* Insulin-like Peptides (DILPs), the fly analog of mammalian insulin [57], into the hemolymph and reduced circulating sugar levels (Figure supplementary 3A). As a result, such manipulation enhanced sweet sensitivity of fed flies (Figure supplementary 3B-C). Therefore, it was plausible that changes in circulating sugar might be the driver of changes in sweet sensation.

Indeed, allowing starved flies to re-feed on normal fly diet or sucrose alone for 15 minutes both resulted in a significant decrease in sweet sensation (Figure 1E). Refeeding with multiple caloric sugars similarly suppressed sweet sensation (Figure Supplementary 4A), indicating that energy intake contributes to the attenuation of sweet sensitivity. To examine whether sweet taste experience itself also plays a role, we refed starved flies with arabinose, a sweet but non-nutritive sugar. Arabinose feeding likewise led to a reduction in sweet sensitivity (Figure Supplementary 4B), suggesting that sweet taste experience can contribute to the suppression of sweet perception, potentially through sensory adaptation. Consistent with this interpretation, responses to other sweet compounds, including trehalose and fructose, were also reduced following sucrose refeeding (Figure supplementary 4C). Conversely, when starved flies were supplied with fly diet deprived of sucrose (but with normal levels of polysaccharides, proteins, and lipids), there was no immediate change in sweet sensation after re-feeding (Figure 1E). These results demonstrate that sugar intake inhibits sweet sensation, probably via increasing circulating sugar levels.

Collectively, we thus hypothesized that the above neuropeptidergic neurons might directly sense an increase of circulating sugar levels and suppress sweet sensation in response. If so, these neurons should be activated by glucose, the main species of circulating sugars associated with feeding behavior in flies [47], at the concentrations resembling sated state (>50 mM in fed flies (Figure supplementary 5)). We thus conducted calcium imaging experiments in fly brains in an *ex vivo* preparation [11]. Among all the six groups of neuropeptidergic neurons we examined in the SEZ, only hugin$^+$ neurons and AstA$^+$ neurons could be activated by 50 mM glucose (Figure 1F-I***, also see*** Figure supplementary 6). Remarkably, each of these populations subdivided into anatomically distinct SEZ subclusters (Figure supplementary 7A; Figure supplementary 9A), yet glucose-evoked Ca^{2+} responses occurred exclusively within a single subcluster (Figure 1H,I; Figure supplementary 7B; Figure supplementary 9B). This selective activation highlighted profound functional heterogeneity in nutrient sensing among these neuron groups. When direct synaptic transmission was blocked with TTX, hugin$^+$ neurons, but not AstA$^+$ neurons, still exhibited calcium responses towards 50 mM of glucose (Figure 1G***, green***), suggesting that hugin$^+$ neurons are a direct glucose sensor. Furthermore, the level of circulating glucose dropped to ~ 20 mM in starved flies (Figure supplementary 5). We found that 20 mM of glucose did not activate hugin$^+$ and AstA$^+$neurons (Figure 1G and I***, orange***), suggesting that these neurons can only be activated under sated conditions.

We also assessed the activity of hugin$^+$ neurons *in vivo* using calcium-modulated photoactivatable ratiometric integrator (CaMPARI), a method employing a photoconvertible fluorescent protein that allows the imaging of integrated calcium activity [58], under both sated and starved conditions. In the CaMPARI assay, when neurons are activated, leading to an increase in free calcium ions, exposure to 405-nm light induces a permanent green-to-red photoconversion [58]. We found an increased ratio of red/green fluorescence in hugin$^+$ neurons in the sated state compared to that upon starvation (Figure 1J). These findings strongly imply that hugin$^+$ neurons function as a direct satiety sensor, sensing the levels of circulating glucose and modulating sweet sensation in response.

Glucose activated hugin$^+$ neurons via an ATP-sensitive potassium channel

We then investigated the cellular mechanism through which glucose could directly activate hugin$^+$ neurons. In both mammals and flies, extracellular glucose is usually transported into the cytosol to activate glucose-sensitive neurons [13,14,59]. When fly brains were pre-treated with phlorizin, a blocker of glucose transport [13,14], hugin$^+$ neurons showed diminished calcium responses to glucose, suggesting activation of hugin$^+$ neurons by glucose requires intracellular glucose (Figure 2A).

The transport of glucose mediated by glucose transporter 1 (Glut1) can activate certain neurons in the fruit fly brain [13,14]. By specifically knocking down Glut1 expression in hugin$^+$ neurons, we observed a significant reduction in calcium responses to glucose (Figure 2B). Consistently, these flies showed a slight yet significant increase in their PER responses to glucose (Figure 2C). Again, these results further confirm that glucose needs to be transported into hugin$^+$ neurons to modulate neuronal activity and behavioral output.

In pancreatic β-cells and certain fly neurons [13,59,60], intracellular glucose modulates cell excitability primarily through its effect on intracellular energy metabolism and ATP-sensitive potassium channels (K_{ATP}). We pre-treated fly brains with a K_{ATP} inhibitor (glibenclamide) and observed a significant calcium response in hugin$^+$ neurons (Figure 2D). Hexokinase, a key enzyme in glucose metabolism that generates ATP, also plays a crucial role in this process. When hexokinase activity was restricted by alloxan, glucose-induced calcium response in hugin$^+$ neurons was significantly suppressed (Figure 2E). Similarly, when hexokinase was specifically knocked down in hugin$^+$ neurons, a comparable reduction in glucose-induced calcium responses was observed (Figure 2F). Pyruvate, the end product from glycolysis, can lead to ATP generation via the tricarboxylic acid cycle. We also found that pyruvate stimulation led to a significant calcium response in hugin$^+$ neurons (Figure 2G). As a specificity control, nonmetabolizable L-glucose failed to activate hugin$^+$ neurons (Figure 2H).

Collectively, these findings suggest that extracellular glucose directly enters hugin$^+$ neurons through specific glucose transporter and subsequently modulate the activity of K_{ATP} through ATP production, ultimately leading to neuronal depolarization. We note that blocking glucose transport or metabolism could, in principle, nonspecifically affect neuronal function, but the rapid and selective nature of the observed responses argues against a generalized loss of excitability.

AstA$^+$ neurons were direct downstream target of hugin$^+$ neurons

Since hugin$^+$ neurons were directly involved in glucose sensing and regulated sweet sensation (Figure 1G and Figure supplementary 8A-B), we sought to identify their downstream target. We then asked whether the hugin peptide had a direct effect on sweet sensation. Upon microinjection of synthetic hugin peptide, we observed a notable reduction in sweet sensation under both sated and starved states (Figure 3A). In line with this observation, following the injection of hugin peptide, we observed a significant reduction of sugar-induced calcium responses in sweet-sensing Gr5a$^+$ neurons (Figure 3B). Thus, the inhibitory function of hugin$^+$ neurons on sweet sensation was likely mediated by the secretion of hugin peptide.

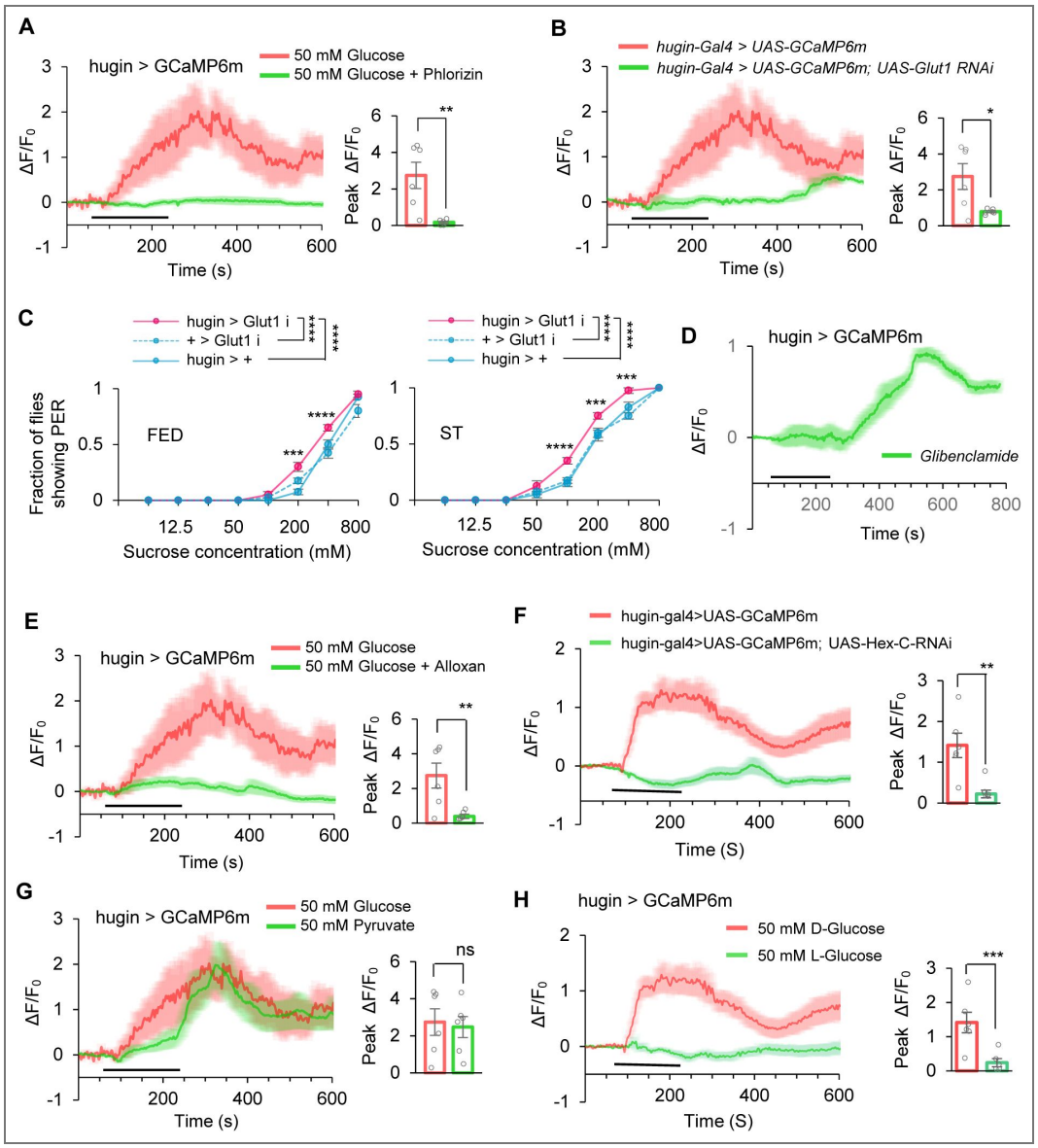

Figure 2. Glucose activated hugin$^+$ neurons via Gltu1 and K_{ATP} channel.

(**A**) Representative traces and quantification of ex vivo calcium responses of hugin$^+$ neurons during the perfusion of glucose with or without phlorizin (1mM, n=6-7). Horizontal black bar represents the duration indicated glucose solution stimulation. (**B**) Representative traces and quantification of ex vivo calcium responses of hugin$^+$ neurons in indicated flies during the perfusion of glucose. (**C**) Fraction of flies of the indicated genotypes showing PER to different concentrations of sucrose (n=4 groups, each of 10 flies). (**D-E**) Representative traces and quantification of ex vivo calcium responses of hugin$^+$ neurons during the perfusion of glibenclamide (100 μM, D), glucose with alloxan (10 μM, E). (**F**) Representative traces and quantification of ex vivo calcium responses of hugin$^+$ neurons in indicated flies during the perfusion of glucose. (**G**) Representative traces and quantification of ex vivo calcium responses of hugin$^+$ neurons during the perfusion of pyruvate (50 mM, n=6). (**H**) Representative traces and quantification of ex vivo calcium responses of hugin$^+$ neurons during the perfusion of D-glucose and L-glucose (50 mM, n=6) ns, P > 0.05; *P < 0.05; **P < 0.01; ****P < 0.0001. Student's t-test and two-way ANOVA followed by post hoc test with Bonferroni correction were used for multiple comparisons when applicable.

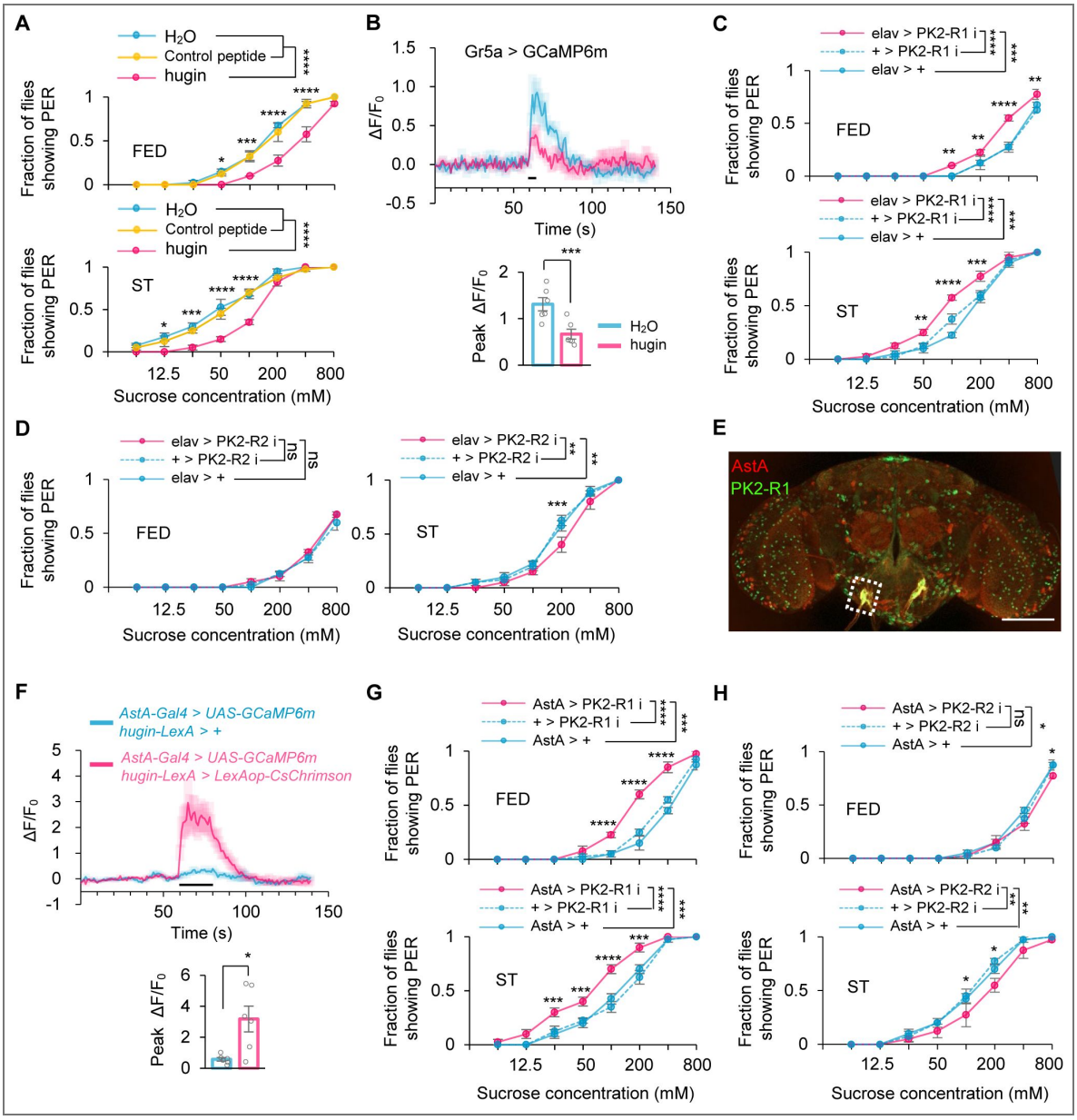

Figure 3. hugin$^+$ neurons activated AstA$^+$ neurons through PK2-R1.

(**A**) Fraction of flies showing PER to different concentrations of sucrose (n=4 groups, each of 10 flies). Flies were injected with saline or synthetic hugin for 30 minutes before the assay. (**B**) Representative traces (upper) and quantification (lower) of peak calcium transients of Gr5a$^+$ neurons in indicated flies upon 5% sucrose after injection of synthetic hugin (n=6). Horizontal black bar represents the duration sucrose stimulation. (**C-D**) Fraction of flies of the indicated genotypes showing PER to different concentrations of sucrose (n=4 groups, each of 10 flies). (**E**) Co-localization (dashed box) of PK2-R1$^+$ neurons (green) and AstA$^+$ neurons (red) in the SEZ region. Scale bar represents 100 μm. (**F**) Representative traces (upper) and quantification (lower) of peak calcium transients of AstA$^+$ neurons after the photo-activation of hugin$^+$ neurons (n=6) from in vivo calcium imaging. Horizontal black bar represents the duration of red-light stimulation. (**G-H**) Fraction of flies of the indicated genotypes showing PER to different concentrations of sucrose (n=4 groups, each of 10 flies). ns, P > 0.05; *P < 0.05; **P < 0.01; ***P < 0.001; ****P < 0.0001. Student's *t-test* and two-way ANOVA followed by post hoc test with Bonferroni correction were used for multiple comparisons when applicable.

There were two hugin receptors, PK2-R1 and PK2-R2, in fruit flies [61]. We knocked down their expression by RNAi in the nervous system and then tested flies' PER to sugar. Knocking down PK2-R1 but not PK2-R2 significantly enhanced sweet perception in both sated and starved states (Figure 3C-D), suggesting a crucial role of PK2-R1 in receiving the input of hugin$^+$ neurons in satiety sensing. To validate this finding, we further tested PK2-R1 null mutants and observed a similar enhancement in sweet sensitivity (Figure supplementary 10). Interestingly, we did not observe any expression of PK2-R1 in the proboscis where gustatory sensory neurons were distributed, indicating that sweet-sensing Gr5a$^+$ neurons could not directly receive input from hugin$^+$ neurons via PK2-R1 (data not shown).

AstA$^+$ neurons served as a plausible relay between hugin$^+$ neurons and sweet-sensing Gr5a$^+$ neurons, especially based on a clear co-expression of hugin receptor PK2-R1 and AstA in the SEZ region of the fly brain (Figure 3E). Notably, these double-labeled neurons corresponded precisely to the AstA subcluster that exhibited glucose-specific Ca^{2+} responses (Figure 1H). We also used optogenetic tools to further confirm that hugin$^+$ neurons acted upstream of AstA$^+$ neurons. We expressed the light-sensitive neuronal activator CsChrimson in hugin$^+$ neurons and calcium indicator GCaMP6m in AstA$^+$ neurons, respectively [62]. As shown in Figure 3F, opto-activation of hugin$^+$ neurons led to a robust calcium transient in AstA$^+$ neurons.

We then investigated whether the hugin-AstA circuitry affected sweet sensation. As expected, knocking-down PK2-R1 (but not PK2-R2) in AstA$^+$ neurons led to a significant increase in sugar-induced PER (Figure 3G-H). Therefore, AstA$^+$ neurons are the direct downstream target of hugin$^+$ neurons in satiety sensing. hugin$^+$ neurons can directly sense elevated circulating glucose levels, promote the release of neuropeptide hugin, and then activate AstA$^+$ neurons via its cognate receptor PK2-R1.

hugin$^+$ neurons are distributed in both the brain and the ventral nerve cord (VNC). The hugin$^+$ neurons in the VNC sense sugar and inhibit feeding behavior by suppressing the activity of DH44 neurons [48]. To determine which hugin$^+$ neurons regulate the activity of AstA neurons and sweet sensation, we performed the following experiments: First, we physically severed the neural connection between the brain and the VNC. Under this condition, activation of Hugin$^+$ neurons still significantly reduced PER responses (Figure Supplementary 11A–B), indicating that hugin$^+$ neurons within the brain are sufficient to modulate sweet perception. Second, in optogenetic experiments using isolated brain preparations, light stimulation of hugin$^+$ neurons elicited robust calcium responses in AstA$^+$ neurons (Figure Supplementary 11C), demonstrating a direct functional coupling between brain Hugin$^+$ neurons and AstA$^+$ neurons.

Notably, comparison of intact and severed preparations revealed that the magnitude of AstA$^+$ neuronal activation was greater when VNC neurons were preserved, suggesting that VNC hugin$^+$ neurons may provide additional modulatory input that enhances AstA activation. Together, these results indicate that Hugin$^+$ neurons in the SEZ constitute a primary pathway linking sugar sensing to AstA activation and PER regulation, while VNC hugin$^+$ neurons contribute to the overall strength of hugin signaling.

AstA$^+$ neurons directly inhibited Gr5a$^+$ neurons

Activation of AstA$^+$ neurons suppressed sweet sensation, resembling the effect of activating hugin$^+$ neurons [17](Figure supplementary 8C-D). We also evaluated the behavioral effect of AstA peptide. Similar to hugin, the microinjection of AstA resulted in a reduction in sweet sensitivity in fruit flies (Figure 4A) and the activity of Gr5a$^+$ neurons (Figure 4B). We then speculated whether AstA$^+$ neurons and AstA peptide might function directly on Gr5a$^+$ neurons. The cell bodies of sweet-sensing Gr5a$^+$ neurons are located in the proboscis, whereas their axons extend to the SEZ region of the fly brain [63]. We observed distributions of the projections of AstA$^+$ neurons and Gr5a$^+$ neurons both in the SEZ region (Figure 4C), suggesting that Gr5a$^+$ neurons might directly receive AstA signal in this region.

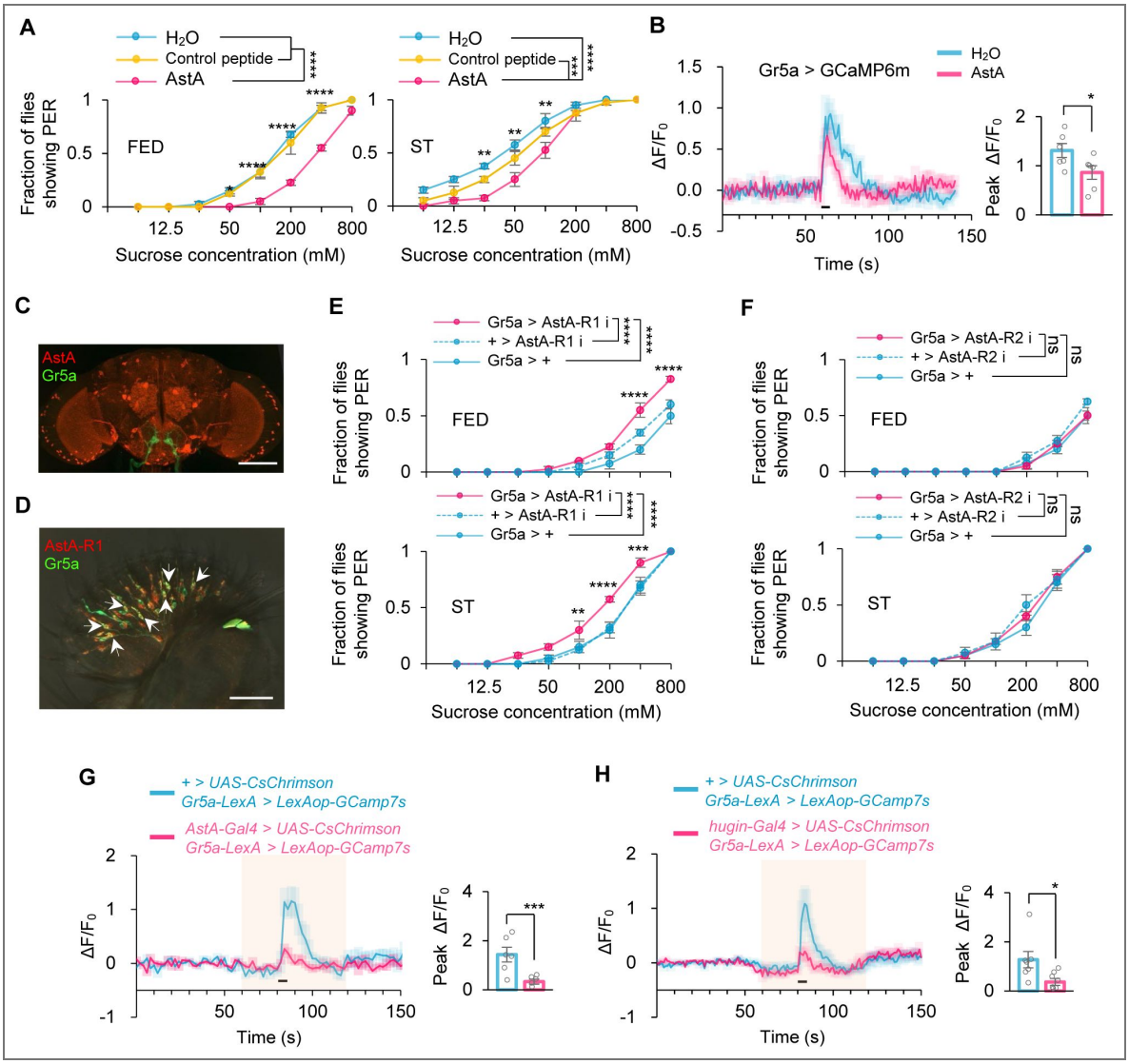

Figure 4. AstA$^+$ neurons inhibited Gr5a$^+$ neurons through AstA-R1.

(**A**) Fraction of flies showing PER to different concentrations of sucrose (n=4 groups, each of 10 flies). Flies were injected with saline or synthetic AstA for 30 minutes before the assay. (**B**) Representative traces (left) and quantification (right) of peak calcium transients of Gr5a$^+$ neurons in indicated flies upon 5% sucrose after injection of synthetic AstA (n=6). Horizontal black bar represents the duration sucrose stimulation. (**C**) Localization of Gr5a$^+$ neurons (green) and AstA$^+$ neurons (red) in the brain. Scale bar represents 100 μm. (**D**) Co-localization of Gr5a$^+$ neurons (green) and AstA-R1$^+$ neurons (red). Arrows point to the neurons co-expressing the two receptors. Scale bar represents 50 μm. (**E-F**) Fraction of flies of the indicated genotypes showing PER to different concentrations of sucrose (n=4 groups, each of 10 flies). (**G-H**) Representative traces (left) and quantification (right) of peak calcium transients of Gr5a$^+$ neurons in indicated flies upon 5% sucrose during the process of photo-activation of AstA$^+$ neurons (G, n=6) and hugin$^+$ neurons (H, n=7-8). Shadows represents the duration of red-light stimulation. Horizontal black bar represents the duration of sucrose stimulation. ns, P > 0.05; *P < 0.05; ***P < 0.001; ****P < 0.0001. Student's *t-test* and two-way ANOVA followed by post hoc test with Bonferroni correction were used for multiple comparisons when applicable.

AstA has two cognate receptors in fruit flies, AstA-R1 and AstA-R2 [64]. Co-labeling experiments in the proboscis confirmed the expression of AstA-R1 in Gr5a$^+$ neurons (Figure 4D, ***arrows***), while AstA-R2 was not expressed in the proboscis (data not shown). Functionally, knockdown of AstA-R1 specifically in Gr5a$^+$ neurons, but not that of AstA-R2, significantly enhanced sweet sensation of flies (Figure 4E-F). Similar results were observed in AstA-R1 knockout flies (Figure supplementary 12).

Using optogenetic tools, we also confirmed the function of hugin$^+$ neurons and AstA$^+$ neurons on Gr5a$^+$ neurons. Activating hugin$^+$ neurons and AstA$^+$ neurons both significantly reduced sugar-induced responses of Gr5a$^+$ neurons (Figure 4G-H). Collectively, these results suggest that satiety-sensing hugin-AstA circuitry can directly modulate sweet sensation of flies via suppressing the activity of Gr5a$^+$ gustatory neurons.

hugin–AstA circuitry suppressed food consumption

Collectively, the hugin-AstA circuitry senses satiety signals and inhibits sweet sensation. Considering the crucial role of sweet sensation in regulating feeding behavior, we hypothesized that hugin-AstA circuitry was also involved in the regulation of food consumption.

We expressed a temperature-sensitive blocker of synaptic transmission (Shibire^{ts1}) in hugin$^+$ neurons or AstA$^+$ neurons [65] and assayed the feeding behavior of flies under both permissive temperature (Figure supplementary 13A, ***blue***) and non-permissive temperature (Figure supplementary 13A, ***red***). In contrast to the suppression of sweet sensitivity observed upon thermogenetic activation of these neurons, silencing hugin$^+$ neurons led to enhanced sweet-driven feeding behavior (Figure supplementary 13B). Consistently, inhibiting synaptic transmission in either hugin$^+$ or AstA$^+$ neurons resulted in a significant increase in food consumption at the non-permissive temperature compared to controls (Figure Supplementary 13C–D).

We also examined the role of hugin and AstA receptors in feeding behavior by testing *PK2-R1* and *AstA-R1* gene knockout flies. The results showed that knockout of both receptors enhanced feeding behavior (Figure supplementary 13E), consistent with increased sweet perception upon genetic manipulation of these two receptors (Figure 3-4). Moreover, these receptor knockout flies exhibited increased lipid storage, which was likely a consequence of their enhanced feeding behavior (Figure supplementary 13F). Additionally, we knocked down the expression of AstA-R1 in sweet sensing Gr5a$^+$ neurons, and found that these flies exhibited a significant increase in food consumption (Figure supplementary 13G), also likely due to the enhanced sweet sensation (Figure 4E).

Mammalian homolog of hugin was also a putative satiety sensor

Our present work identified hugin-AstA circuitry as a novel satiety sensor and feeding suppressor in fruit flies. Fruit flies and mammals share highly conserved regulatory elements on feeding behavior and energy homeostasis [51,66,67]. We thus asked whether this novel satiety-sensing mechanism was also conserved in the mammalian system,

In rodent models, neuromedin U (NMU), a analogues of hugin, was also found to be an appetite suppressor [15,18]. We found that synthetic NMU could suppress sweet perception when injected into flies' thorax (Figure supplementary 14), highlighting the analogy of fly hugin and mammalian NMU. In mouse models, we observed a significant increase in NMU levels in the blood following glucose feeding (Figure 5A). Using the sucrose preference test (SPT) to measure sweet preference, we noted that NMU injection reduced sugar preference in mice, phenocopying the effect of glucose feeding (Figure 5B-C). Conversely, NMU knockout enhanced sweet sensation in mice (Figure 5D). These data demonstrated that both NMU gene and protein plays a crucial role in regulation of sweet sensation.

Neuropeptide NMU is secreted by a group of neurons located in the VMH region of hypothalamus [18]. To investigate whether NMU$^+$ neurons functioned as an energy sensor in the mouse brain, we injected AAV-EF1α-DIO-GCaMP6m-WPRE into the VMH of NMU-Cre mice, specifically expressing GCaMP6m in NMU$^+$ neurons. We then monitored the dynamic activity of VMH ^{NMU} neurons

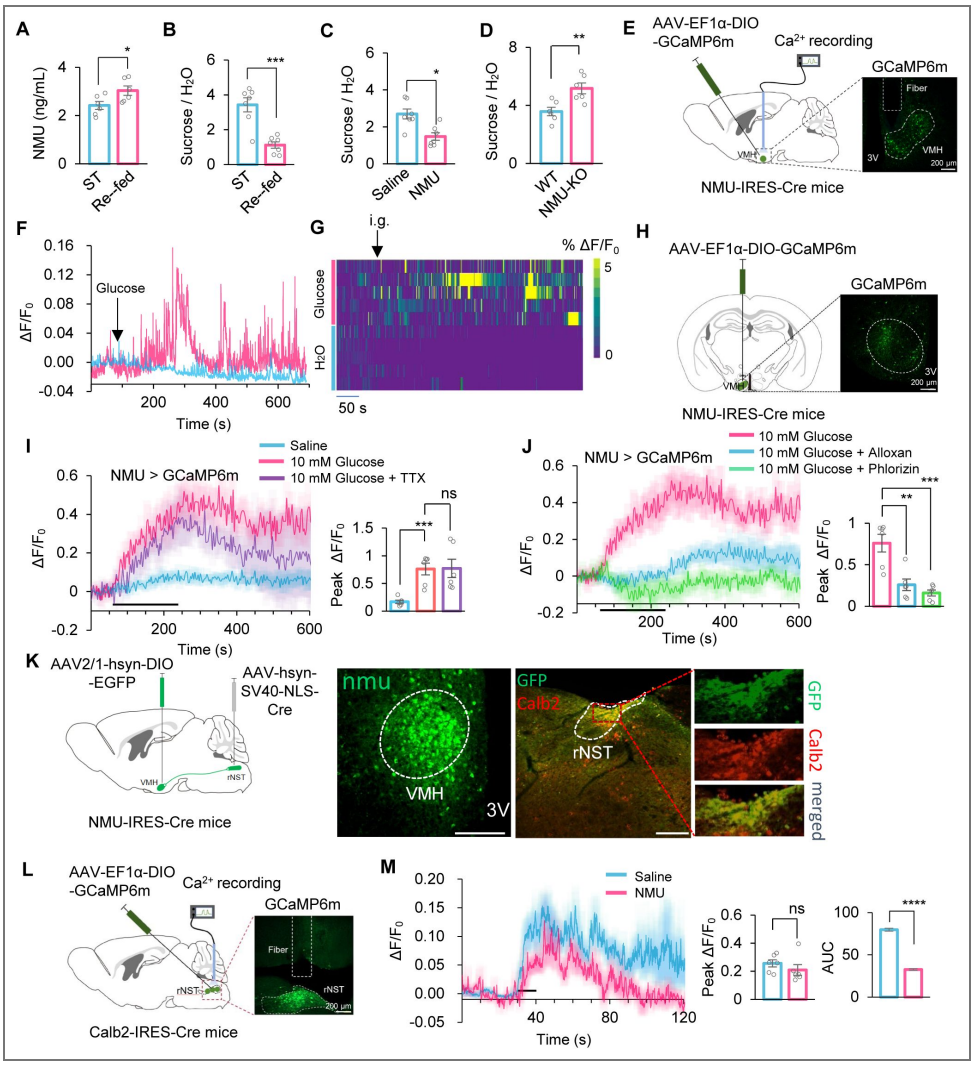

Figure 5. NMU$^+$ neurons were the central energy sensor in mouse.

(**A**) Blood NMU levels of starved mice re-fed with 20% sucrose (n=6). (**B**) Two-bottle preference tests for starved mice re-fed with sucrose (n=7). (**C**) Two-bottle preference tests for starved mice with or without intraperitoneal injection of NMU peptide (YFLFRPRN-NH_2, 4.5μm/kg) (n=7). (**D**) Two-bottle preference tests for indicated starved mice. (**E**) Fiber photometry to record the calcium dynamics of NMU$^+$ neurons in the VMH with GCaMP6m (left) and representative IHC image of expressing GCaMP6min VMH (right). (**F-G**) Representative trace (left) and heatmaps (right, n=5) showing calcium dynamics of NMU$^+$ neurons in the VMH in response to gastric glucose infusion (20% sucrose, 200 μl), which elevates circulating glucose levels independently of oral sensory stimulation.. (**H**) Experimental approach to assess calcium signaling in NMU$^+$ neurons in the VMH in vitro (left) and representative IHC image of expressing GCaMP6min VMH (right). (**I-J**) Representative traces and quantification of ex vivo calcium responses of NMU$^+$ neurons during the perfusion of glucose with or without TTX (I), Alloxan (J) and Phlorizin (J) (n=6-7). Horizontal black bar represents the duration indicated glucose solution stimulation. (**K**) **Anterograde trans-synaptic tracing of downstream targets of NMU$^+$ neurons.** NMU$^+$ neurons were labeled by GFP expression following injection of a Cre-dependent AAV2/1-DIO-GFP into NMU-Cre mice. This virus undergoes anterograde trans-synaptic transfer to postsynaptic neurons. To enable GFP expression specifically in downstream target regions, an AAV-Cre virus was locally injected into the rNST. As a result, postsynaptic neurons in the rNST receiving input from NMU$^+$ neurons were labeled by GFP delivered anterogradely from upstream NMU$^+$ neurons. Representative images show that GFP-labeled downstream neurons in the rNST colocalize with Calb2 immunoreactivity, indicating that NMU$^+$ neurons preferentially target Calb2$^+$ rNST neurons. (**L**) Fiber photometry to record the calcium dynamics of Calb2$^+$ neurons in the rNST with GCaMP6m (left) and representative IHC image of expressing GCaMP6m in rNST (right). (**M**) Representative traces and quantification of calcium responses of Calb2$^+$ neurons during glucose licking under physiological feeding conditions (500 mM sucrose), with or without NMU administration, assessing downstream modulation of sweet-responsive brainstem circuits. ns, P > 0.05; *P < 0.05; **P < 0.01; ***P < 0.001; ****P < 0.0001. Student's *t-test* and one-way ANOVA followed by post hoc test with Bonferroni correction was used for multiple comparisons when applicable.

during glucose stimulation by using fiber photometry (Figure 5E). As expected, these neurons showed significant calcium responses following glucose administration in mice (Figure 5F-G). To confirm the specificity of GCaMP6m expression in NMU^+ neurons, we co-expressed a Cre-dependent mCherry reporter in the VMH of NMU-Cre mice and performed fluorescence in situ hybridization for NMU mRNA. Colocalization analysis demonstrated that GCaMP6m fluorescence was restricted exclusively to NMU^+ cells (Figure supplementary 15A).

Next, we conducted calcium imaging of brain slices *in vitro* to further assess these neurons' ability to sense glucose (Figure 5H). Similar to hugin neurons in the fly brain, VMH^{NMU} neurons in the mouse brain exhibited strong calcium responses to glucose stimulation, which could not be inhibited by TTX (Figure 5I), indicating their direct glucose-sensing capability. Also similar to flies, glucose activated these mouse neurons via entering the cells and modulating K_{ATP} channels, as evidenced by the inhibition of calcium responses by alloxan and phlorizin (Figure 5J). While supraphysiological glucose concentrations were used in slice recordings to ensure reliable neuronal activation under ex vivo conditions, complementary in vivo recordings demonstrate that VMH NMU^+ neurons are engaged by physiological sugar ingestion.

Calbindin 2-positive neurons (Calb2) in the rostral nucleus of the solitary tract (rNST) selectively respond to sweet tastants, facilitating sweet signal from the periphery into the brain [68]. Because attenuated sweet sensation should correspondingly diminish central sweet-signal transmission, we asked whether NMU modulates this relay. To assess potential anatomical connectivity between VMH NMU^+ neurons and rNST $Calb2^+$ neurons, we employed a dual-virus tracing strategy. In NMU-Cre mice, we injected AAV9-EF1α-DIO-EGFP into the VMH, which revealed dense GFP^+ projections in close apposition to $Calb2^+$ neurons in the rNST (Figure supplementary 15B). To further confirm this projection is monosynaptic, we combined anterograde tracing by co-injecting AAV2/1-EF1α-DIO-EGFP into the VMH and AAV2/1-hsyn-SV40-NLS-Cre into the rNST. This approach yielded GFP expression in rNST $Calb2^+$ neurons, supporting a direct VMH → rNST NMU^+ → $Calb2^+$ synaptic link (Figure 5K).

To evaluate the functional consequence of NMU on $Calb2^+$ neuronal activity during sweet stimulation, we delivered AAVs encoding Cre-dependent GCaMP6m into the rNST of Calb2-Cre mice, thereby enabling real-time calcium imaging in $Calb2^+$ neurons (Figure supplementary 15C). Using fiber photometry, we recorded calcium responses to sugar stimuli, both with and without NMU injection (Figure 5L). We found that NMU injection elicited a significant, albeit partial, suppression of calcium responses to sugar (Figure 5M). Although the magnitude of this reduction was modest compared to the complete silencing of activity, the effect was statistically robust and aligned with the behavioral phenotypes, indicating that NMU acts to dampen sweet taste perception during feeding.

These findings indicate that NMU^+ neurons can indeed be a putative satiety sensor in the mouse brain that suppresses sweet perception, shedding light on understanding the conserved neural mechanism of feeding regulation in mammals including human.

Discussion

In this study, we identify a neural pathway that directly couples internal glucose levels to the regulation of sweet taste perception and feeding behavior. In *Drosophila*, circulating glucose activates a specific subset of hugin neurons, which signal to AstA neurons to suppress the activity of peripheral sweet-sensing Gr5a neurons, thereby reducing sweet sensitivity and terminating feeding. This pathway establishes a direct neural link between internal energy state and early sensory processing.

A notable feature of this circuit is that its manipulation produces significant but relatively modest changes in sweet sensitivity compared with the dramatic enhancement observed under starvation[52,69]. This difference reflects the distinction between a specific satiety mechanism and the global physiological state of hunger. Starvation is a systemic crisis that engages multiple hunger-promoting pathways, including dopaminergic and NPF signaling, which broadly elevate motivational drive and sensory gain[10,70]. In contrast, the hugin–AstA pathway functions as a

glucose-dependent inhibitory branch—a "satiety brake"—that is selectively engaged in fed states to dampen sweet sensation. Disrupting this inhibitory pathway prevents full suppression of sweet sensitivity after feeding but does not recreate the potent hunger drive generated by dopaminergic activation. Thus, energy homeostasis arises from the coordinated action between hunger accelerators and satiety brakes.

This framework reconciles our findings with previous reports that silencing hugin neurons does not alter proboscis extension in starved flies[20]. Under starvation, hugin neuronal activity is already physiological low due to reduced circulating glucose, meaning the "brake" is already released. Consequently, further silencing has little additional effect. In contrast, preventing the starvation-induced reduction of hugin activity—such as by thermogenetic activation—significantly suppresses hunger-enhanced sweet sensitivity. These results indicate that the dynamic downregulation of hugin neuron activity is a critical component of the state-dependent modulation of taste.

Our data further reveal functional heterogeneity within peptidergic populations. Although hugin and AstA neurons are broadly distributed in the central nervous system (including the subesophageal zone and ventral nerve cord), only specific subpopulations respond to elevated glucose[43,48]. While descending inputs from the VNC may potentiate signaling, our data suggest that the glucose-responsive hugin neurons in the SEZ constitute a dedicated energy-sensing module. This heterogeneity likely explains both the partial behavioral effects of global manipulations and the ability of hugin neurons to regulate diverse behaviors beyond feeding, such as locomotion.

Circulating sugars represent a complex internal signal. In *Drosophila*, trehalose serves as the major circulating sugar supporting stress resistance, whereas glucose functions as the primary, rapidly mobilized energy substrate[71]. Unlike receptor-based sensors (e.g., Gr43a for fructose)[72], Hugin neurons rely on intracellular glucose metabolism and K^{ATP} channel activity to modulate neuronal excitability. This mechanism ensures that the circuit activity is tightly coupled to cellular energy status. Consistent with this, feeding with fructose, trehalose, or non-nutritive sweeteners only weakly suppressed sweet sensitivity within the acute post-feeding interval, whereas sucrose —which rapidly restores hemolymph glucose—robustly activated this pathway. Thus, our work identifies glucose as the key metabolic signal that engages this central brake.

The presence of multiple sugar-sensing systems in *Drosophila* reflects functional specialization rather than redundancy. Peripheral and gut-derived signals regulate feeding over longer timescales, while central hunger circuits adjust sensory gain during deprivation. The hugin–AstA circuit adds a distinct layer by acting as a rapid central brake that prevents overconsumption when energy stores are sufficient.

Strikingly, we find that this circuit logic is conserved in mammals. Although NMU has been implicated in feeding suppression[73,74], whether NMU neurons sense internal nutrients directly had remained unclear. Our data demonstrate that VMH NMU^{+} neurons are activated by elevations in internal glucose and form a functional circuit with sweet-responsive Calb2 neurons in the rostral nucleus of the solitary tract (rNST). Gastric glucose infusion experiments established that NMU neurons respond to internal metabolic signals independently of oral sensory input, while physiological sugar ingestion confirmed that this pathway actively suppresses downstream sweet-driven activity. Together, these findings define a previously unrecognized NMU-centered circuit linking internal glucose sensing to the modulation of early taste processing. All mouse experiments in this study were performed in male animals; whether sex-specific differences exist in NMU-mediated glucose sensing and taste modulation remains an important question for future investigation.

The conservation of this "satiety brake" suggests that suppressing sensory gain via central neuropeptidergic energy sensors is a fundamental strategy for maintaining energy balance. By defining a direct link between internal glucose levels and sweet taste perception, our work provides a mechanistic framework for understanding how metabolic state shapes sensory experience and feeding behavior.

Materials and methods

Animals

Fly: Flies were maintained on a standard fly diet under conditions of 60% humidity and 25 °C with a 12-hour light and 12-hour dark cycle. Virgin female flies were chosen immediately after emerging and housed in standard fly food (ND) vials, with 20 flies per vial, for a period of 5-6 days before experiments. For temperature-sensitive manipulations (dTrpA1, Shibire^{ts}), flies were reared at 18 °C for 7–8 days, then transferred to 30 °C for 30 min to activate or inhibit targeted neurons; behavioral assays (PER or feeding) were conducted continuously at 30 °C. For starvation, the flies were kept on 2 % Agar for 12-hour. For refeeding, the fasted flies were transfer to different food for 15 mins.

The following UAS-RNAi lines: *UAS-AstA-R1 RNAi* (#27280), *UAS-AstA-R2 RNAi* (#25935), *UAS-PK2-R1 RNAi (#29624)*, *UAS-PK2-R2 RNAi (#28781)*, *UAS-CD8-GFP, LexAop-CD2-RFP (#67093)*, *UAS-GCaMP6m* (*#42748*), *UAS-CaMPARI* (*#58764*), *Gr5a-GAL4* (*#57592*), *Gr5a-LexA* (#93014), *ilp2-GAL4 (#37516)*, *elav-GAL4 (#25750)* were obtained from the Bloomington Drosophila Stock Center at Indiana University. *TH-KO*, *PK2-R1-KO*, *AstA-R1-KO* and all the other Gal4 and LexA lines (*AstA-Gal4, LK-Gal4, hugin-Gal4, TK-Gal4, CCHa1-Gal4, CCHa2-Gal4, TH-Gal4, PK2-R1-Gal4, AstA-LexA, AstA-R1-LexA*) were from Yi Rao (Deng et al., 2019) (Capital Medical University, Beijing). *UAS-dTrpA1* and *UAS-Shibire^{ts1}* were from David Anderson (Caltech). *UAS-GCaMP6m; LexAop-CsChrimson* was from Yufeng Pan (Southeast University, Nanjing). *LexAop-Chrimson* was from Wei Zhang (Tsinghua University, Beijing).

Mouse: Male C57BL/6J mice at the age of four weeks were procured from cyagen. The mice were kept in standard laboratory conditions at a temperature of 25 °C with a 12:12 light/dark cycle. All experimental procedures were conducted in compliance with the guidelines set by the Laboratory Animal Welfare and Ethics Committee of Chongqing University (CQU-IACUC-RE-202401-004), adhering to both national and international standards.

Behavioral assays (Fly)

PER was evaluated using a method outlined in a previous study. Briefly, individual flies were gently aspirated and positioned in a 200 μL pipette tip, allowing only the head and proboscis to protrude while the dorsal thorax was lightly affixed to prevent escape. After a 3-minute acclimation period, each fly was first presented with 0.5 μL water droplets on the labellum twice. Flies that responded by extending their proboscis were allowed to drink and were subsequently excluded from the experiment. Flies that did not extend their proboscis in response to water were then stimulated sequentially with ascending sucrose concentrations (6.25–800 mM). Each concentration was delivered as two brief (<1 s) touches of a 0.5 μL droplet to the labellum, immediately withdrawn to prevent ingestion. A full proboscis extension, defined as the complete uncoiling of the rostrum beyond the labellum plane, was scored as positive. Partial or delayed (>1 s) extensions were not considered positive responses. Responsiveness at each concentration was recorded if at least one full extension occurred in the two trials.For Figure supplementary 11, the connection between the brain and VNC were cut off by a dissecting scissors before the PER assay.

Feeding was assessed as previously described [78]. Briefly, 5-day-old flies underwent a 12-hour starvation period on 2% agar and were then moved to a new vial with test food containing 0.5% Brilliant Blue (MACKLIN, China) for 10 minutes. After a rapid freeze at −20 °C, flies were decapitated in PBS, homogenized, and centrifuged (13,000 g * 5 min). The resulting supernatants were diluted with PBS to a total volume of 1 ml, and absorbance was measured at 620 nm.

Sucrose Preference Test

The two-bottle preference (TBP) behavioral test was conducted in a standard mouse cage. Two bottles, one containing water and the other with a 10 mM sucrose solution, were placed on top of the cage. Each tested mouse was individually caged and adopted to two bottles containing distilled

water or a 10 mM sucrose solution for one week. Throughout the training period, the positions of the bottles were alternated every 24 hours to mitigate potential position-related biases. Prior to the TBP tests for sucrose, mice underwent a 12-hour pre-starvation period, followed by re-fed sucrose (20%) for 1 hour or intraperitoneal (IP) administration of NMU (YFLFRPRN-NH_2, 4.5 μm/kg). The consumption of water and sucrose solution over a 2-hour period was meticulously recorded. The sweetener preference ratio was then calculated by dividing the weight of sweetener consumed by the weight of water consumed.

NMU measurement

Blood was obtained from the lower jaw of the mice and clotted at room temperature for 1 hour. The samples were then centrifuged (1,500g, 4 °C) for 10 minutes and the supernatants were collected for NMU measurement. All the manipulations were according to the manufacturer's instructions (BMASSY,74030).

Hemolymph extraction and glucose measurement

Groups of 40 ice-anesthetized flies were decapitated and placed into a perforated 0.5 ml tube, which was nested inside a 1.5 ml collection tube. Samples were centrifuged at 2,500 × g for 10 min at 4 °C, yielding approximately 2 μl of hemolymph per batch. Hemolymph was pooled to 4 μl per assay (n = 8 independent samples per group) and immediately analyzed for glucose concentration using the Solarbio BC2500 kit (Solarbio, China) according to the manufacturer's instructions.

Microinjection

Flies were delicately positioned and secured within a 200 ml pipette tip, ensuring their heads were directed toward the tip's end. Subsequently, the tip was opened by cutting, exposing the heads and a section of the thorax. About 20 nl of sterile saline, either with or without synthesized peptides (hugin: SVPFKPRL-NH_2, 1 mg/ml (1.1 mM); AstA: LPVYNFGL-NH_2, 1mg/ml (1.1 mM); NMU: YFLFRPRN-NH_2, 1mg/ml (0.9 mM); Control peptide: DYKDDDDKYPYDVPDYA, 1mg/ml (0.48 mM), were injected into the thorax of these flies using a glass micropipette and a microinjector (3-000-207, Drummond Scientific Company Instruments). The glass micropipette was created from thick-walled borosilicate capillaries (3-000-203-G/X, Drummond Scientific Company Instruments).

Immunofluorescence staining

Fly brains were carefully dissected in PBS on ice and then fixed in 4% formaldehyde for 60 minutes. Following fixation, the brains underwent permeabilization and blocking using Dilution/Blocking Buffer (PBS containing 10% Calf Serum and 0.5% Triton X-100) for 2 hours at room temperature. Subsequently, the samples were immersed in the appropriate primary antibodies in Dilution/Blocking Buffer for 24 hours at 4 °C. Afterward, the samples were subjected to a 60-minute wash with Washing Buffer (0.5% Triton X-100 in PBS) four times at room temperature and were then incubated with secondary antibodies for 24 hours at 4 °C. The samples underwent three additional washes with Washing Buffer before being mounted in Fluoroshield (Sigma-Aldrich).

Images were acquired using a scanning confocal microscope with Olympus objectives (20× /0.7 and 40× /0.95w). Antibodies were employed at the following dilutions: mouse anti-nc82 (1:100, DSHB), rabbit anti-GFP (1:500, Abcam), Alexa Fluor 647 goat anti-mouse (1:500, Invitrogen), and Alexa Fluor 488 goat anti-rabbit (1:500, Invitrogen).

In situ hybridization

Mice were anesthetized and perfused with 4% paraformaldehyde (PFA) dissolved in phosphate-buffered saline (PBS, pH 7.4). Brains were carefully removed from the skull and post-fixed in 4% PFA at 4 °C overnight. Subsequently, the brains were transferred to a 20% sucrose solution (in 1 × PBS) at 4 ° C until they were ready for sectioning. Twenty-micrometer-thick sections were obtained using a cryostat. The detection of nmu was performed using a fluorescent in situ hybridization technique (RNAscope, Pinpoease) according to the manufacturer's instructions. Sections were

mounted on SuperFrost Plus Gold slides (ThermoFisher) and briefly rinsed in autoclaved Millipore water. They were then subjected to gradient dehydration in 50%, 75%, and 100% ethanol for 5 minutes each. A hydrophobic barrier was created around the sections using an ImmEdge hydrophobic barrier pen (Cat No. 310018). All incubation steps were carried out at 40 °C using the Pinpoease hybridization system (Cat No. SH-08). The subsequent hybridization, amplification, and detection steps were performed strictly according to the manufacturer's instructions.

Stereotaxic brain surgeries and viral injection

Mice were anesthetized with 1-2% isoflurane during stereotaxic injections, performed using a small animal stereotaxic instrument (RWD Life Science, #68030). Throughout the surgery, core body temperature was maintained at 36 ± 1 °C using a feedback-controlled heating system. Micro scissors were used for the incision, and a dental drill was employed to create the cranial window. Viral injections were delivered using a glass microelectrode syringe pump (RWD Life Science, #R-480). To express GCaMP6m and mCherry AAV2/9-EF1α-DIO-GCaMP6m-WPRE (titer: 2.89×10^{12}, #H4955, Obio Biotechnology, Shanghai, China, Co., Ltd.) and AAV2/9-EF1α-DIO-mCherry-WPRE (titer: 2.89×10^{12}, Obio Biotechnology, Shanghai, China, Co., Ltd.) were bilaterally injected into the VMH and rNST, with approximately 0.15 μL of virus delivered per site. The microelectrode was left in place for 10 minutes post-injection before being withdrawn. Injection coordinates were as follows: VMH (AP, −1.46 mm; ML, ±0.4 mm; DV, −5.5 mm) and rNST (AP, −7.08 mm; ML, ±0.6 mm; DV, −4.3 mm). After 3 weeks of AAV injections, optical fibers were chronically implanted in the VMH or rNST and secured with dental cement (C&B Metabond®, Parkell, Japan). Injection coordinates were determined based on the 4th edition of the mouse brain atlas by Franklin and Paxinos (2008). Mice were allowed to recover for 5-7 days post fiber-implanted before any behavioral or calcium imaging evaluations were conducted. After the experiments, mice were perfused to verify virus expression and fiber placement. Data from mice with poor viral expression or incorrect fiber placement (0-20% of cases) were excluded from the final analysis.

For the anterograde tracing experiments, two viral vectors were used. AAV2/1-hsyn-DIO-EGFP-WPRE (titer: 1×10^{13} viral particles/mL,Obio Biotechnology) was injected into the ventromedial hypothalamus (VMH), and AAV2/1-hsyn-SV40 NLS-Cre (titer: 2.1×10^{12} viral particles/mL, Brain Case) was injected into the rostral nucleus of the solitary tract (rNST). Approximately 0.15 μL of virus was delivered per injection site. After 3 weeks, the brains were perfused and fixed. Subsequently, the brain tissues were sliced and subjected to antibody staining. The fluorescence signals were then recorded and analyzed.

Optical-fiber-based calcium recording in freely mice

Following injection of an AAV2/9-EF1α-DIO-GCaMP6m-WPRE viral vector, an optical fiber (200μm O.D., 0.37 numerical aperture, Inper Inc., China) was placed 150 μm above the viral injection site. GCaMP6m$^+$ mice were implanted with the optic fiber 3 weeks post-AAV injection and allowed to recover for 5–7 days prior to experimental testing.

For Figure 5K-L, six mice were first trained to lick glucose (500 mM) from a petri dish. After training, they were fasted for 12 hours and then received an intraperitoneal injection (ip) of synthetic NMU peptide (4.5 μm/kg), followed by a 30-minute waiting period. During the experimental session, the mice were given 10 seconds to lick glucose from the petri dish while undergoing fiber photometry recording. For Figure 5E-G, mice were fasted for 4 hours and then administered glucose via gastric infusion, with fiber photometry recordings capturing the process. Fluorescence signals were acquired using a dual-channel fiber photometry system (410 nm & 470 nm, RWD Life Science). The laser power at the tip of the optical fiber was kept below 20 μW for both the 470 nm and 410 nm channels to minimize bleaching. ΔF / F was calculated as (470 nm signal - fitted 410 nm signal) / fitted 410 nm signal. Data analysis was performed using software from RWD Life Science.

Ex vivo calcium imaging

For Figure 1G, 1I, figure supplementary 6, and Figure 2 freshly dissected fly brains were placed in the sugar-free AHL buffer (108 mM NaCl, 8.2 mM $MgCl_2$, 4 mM $NaHCO_3$, 1 mM NaH_2PO_4, 5 mM KCl, 2 mM $CaCl_2$, 5 mM HEPES, pH 7.3). Baseline recordings of the samples in AHL buffer were taken over 1 minutes. Subsequently, the solutions were added with 100 μM glibenclamide (Figure 2D), 50 mM pyruvate (Figure 2G) or switched to AHL + glucose (50 mM) with or without indicated chemicals (Figure 2 A and E, 1 mM phlorizin or 10 um alloxan), and the pH was adjusted back to 7.3 through gentle perfusion for 3 minutes. Solution flow in the perfusion chamber was controlled by a valve commander (Scientific Instruments). Following stimulation, samples were washed out again with AHL. For the TTX test, 2 μM TTX was added to the AHL solution. Prior to the assay, the samples were pre-treated with 2 mM TTX for 15 minutes.

For Figure 5H-J, mice (6-9 weeks of age) were deeply anesthetized by avertin (1.25% avertin, 0.2 ml/10g). Mouse brains were quickly extracted following decapitation and immediately placed in ice-cold slicing buffer (110 mM Choline Cl, 2.5 mM KCl, 1 mM NaH_2PO_4, 25 mM $NaHCO_3$, 5 mM glucose, 7 mM $MgCl_2$, 0.5 mM $CaCl_2$,1.3mM Na ascorbate,0.6mM Na pyruvate bubbled with 95% oxygen and 5% CO_2 with an adjusted pH of 7.3). The brains were then sectioned into 200 μm slices using a vibratome (Leica VT1200S). These slices were incubated artificial cerebrospinal fluid (aCSF) (125 mM NaCl, 2.5 mM KCl, 1 mM NaH_2PO_4, 25 mM $NaHCO_3$, 5 mM glucose, 1.3 mM $MgCl_2$, 2 mM $CaCl_2$,1.3mM Na ascorbate, 0.6 mM Na pyruvate bubbled with 95% oxygen and 5% CO_2 with an adjusted pH of 7.3) at 34 °C for 20 minutes, then transferred to a room temperature for 30 minutes before recording. For Ca^{2+} imaging, the slices were placed in a recording chamber in the low sugar aCSF (125 mM NaCl, 2.5 mM KCl, 1 mM NaH_2PO_4, 25 mM $NaHCO_3$, 1 mM glucose, 1.3 mM $MgCl_2$, 2 mM $CaCl_2$, 1.3 mM Na ascorbate, 0.6mM Na pyruvate, pH 7.3) for 10 minutes (maintained the flow rate for 1-3 ml/ minute). Baseline recordings, perfusion, and Ca^{2+} recording were performed as detailed above.

All imaging was conducted on an Olympus confocal microscope (FVMPE-RS) with a water immersion objective lens (25× /1.05w MP). Image analyses were performed using ImageJ to calculate the mean intensity of the indicated neuron targeting ROIs, and then plotted in Excel (Microsoft). Ratio changes were calculated using the formula: $\Delta F / F = [F - F_0] / F_0$, where F represents the mean fluorescence of the cell body, and F_0 is the average baseline (before stimulation).

Optogenetics and in vivo calcium imaging

Newly emerged virgin female flies were housed in a fresh vial with standard medium for 3 days and subsequently moved to a vial containing regular food supplemented with 400 μM all-trans-retinal (Sigma R2500) for 2-4 days prior to experiments. These flies were then immobilized on ice, affixed to transparent tape, and the dorsal cuticle of the fly head was delicately removed with forceps to expose the brain, which was immersed in AHL.

For Figure 3F, an array of red LED (Thorlabs, M625L3) was positioned above the brain. Calcium signals of $Gr5a^+$ neurons were captured for 60 frames (1 second per frame) in the absence of light to establish a baseline. Subsequently, the next 20 frames were recorded during opto-activation with the light (the light was switched on for 0.45 second and rested for 0.55 second per activation cycle, and the images were collected in rest time), followed by another 60 frames recorded without light afterward.

For Figure 4G and 4H, to apply liquid food (5% sucrose) to the proboscis, a pipette was filled with the taste solution and placed a few microns from the proboscis tip by using a micromanipulator (MP225, Sutter Instruments) prior to recording. Then, we recorded calcium signals for 60 seconds in the absence of light to establish a baseline (1 second per frame). To activate neurons expressing CsChrimson, a red LED was positioned above the brain, controlled by a custom computer program during opto-activation (0.45 second on and 0.55 second off from 60 second to 120 second). The pipette was placed on the proboscis from 80 second to 85 second. Calcium signals of $Gr5a^+$ neurons were recorded throughout these processes (1 second per frame).

Image analyses about relative fluorescence changes ΔF / F were performed as ex vivo calcium imaging.

Optogenetics and ex vivo calcium imaging

For Figure supplementary 11C, newly emerged virgin female flies were housed in a fresh vial with standard medium for 3 days and subsequently moved to a vial containing regular food supplemented with 400 μM all-trans-retinal (Sigma R2500) for 2-4 days prior to experiments. The brains were dissected and placed under a red LED. Calcium signals of AstA$^+$ neurons were recorded with or without LED light as above. Image analyses were performed as ex vivo calcium imaging.

Calcium imaging with CaMPARI

The flies were then gently immobilized on ice, attached to transparent tape, and the dorsal cuticle of the fly head was carefully removed with forceps to expose the brain, which was immersed in AHL. Photoconversion (PC) was achieved for 30 seconds using a 405 nm LED [Thorlabs, M405L2–UV (405 nm) Mounted LED, 1,000 mA, 410 mW], controlled by a LED controller (Thorlabs, LEDDB1 driven with 1000 mA). Images were captured using an Olympus confocal microscope. Image analyses were performed in ImageJ by manually drawing ROIs covering individual neuronal cell bodies using the green channel. The extent of CaMPARI photoconversion was determined as the Red: Green ratio.A '-405 nm' control was included to demonstrate that scanning of the hugin neurons without exposure to ultraviolet light does not convert green to red fluorescence.

Statistical analysis

Data are shown as means (± SEM). Data presented in this study were verified for normal distribution by D'Agostino–Pearson omnibus test. Student's t test, one-way ANOVA and two-way ANOVA (for comparisons among three or more groups and comparisons with more than one variant) were used. The post hoc test with Bonferroni correction was performed for multiple comparisons following ANOVA.

Supplementary figures

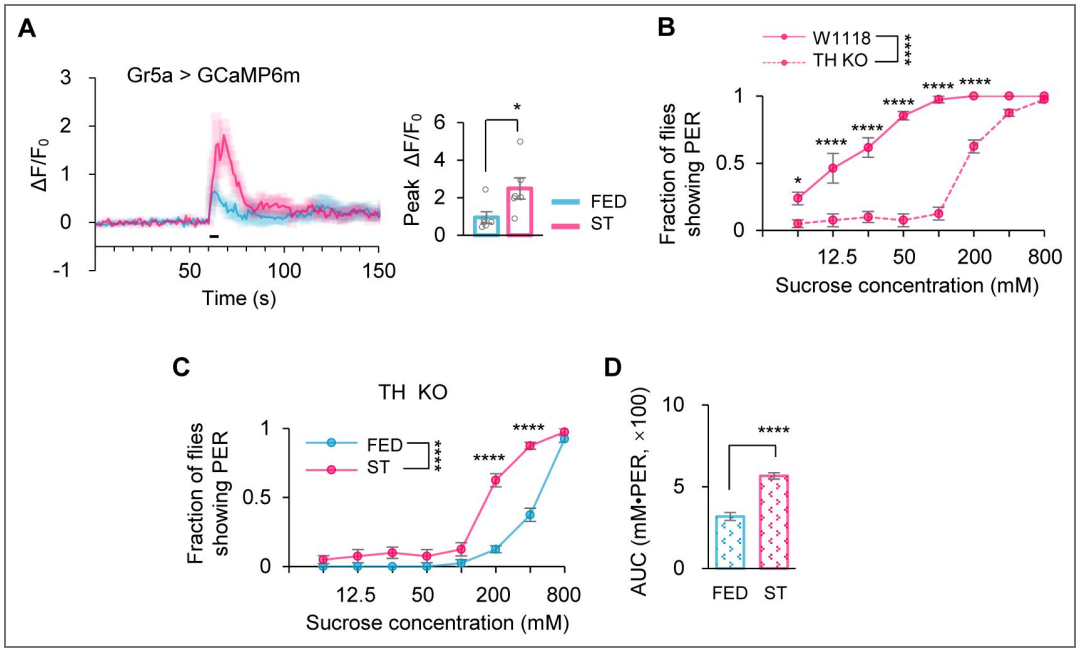

Figure supplementary 1. Satiety suppressed sweet sensitivity in a dopamine-independent manner. (**A**) Representative traces (left) and quantification (right) of peak calcium transients of Gr5a$^+$ neurons in indicated flies (n=6). Horizontal black bar represents the duration 5% sucrose stimulation. (**B-D**) Fraction of flies of the indicated

genotypes showing PER to different concentrations of sucrose (B-C, n=4 groups, each of 10 flies). The Area Under the Curve (AUC, D) represents sweet sensitivity in C. *P < 0.05; ****P < 0.0001. Student's *t-test* and two-way ANOVA followed by post hoc test with Bonferroni correction were used for multiple comparisons when applicable.

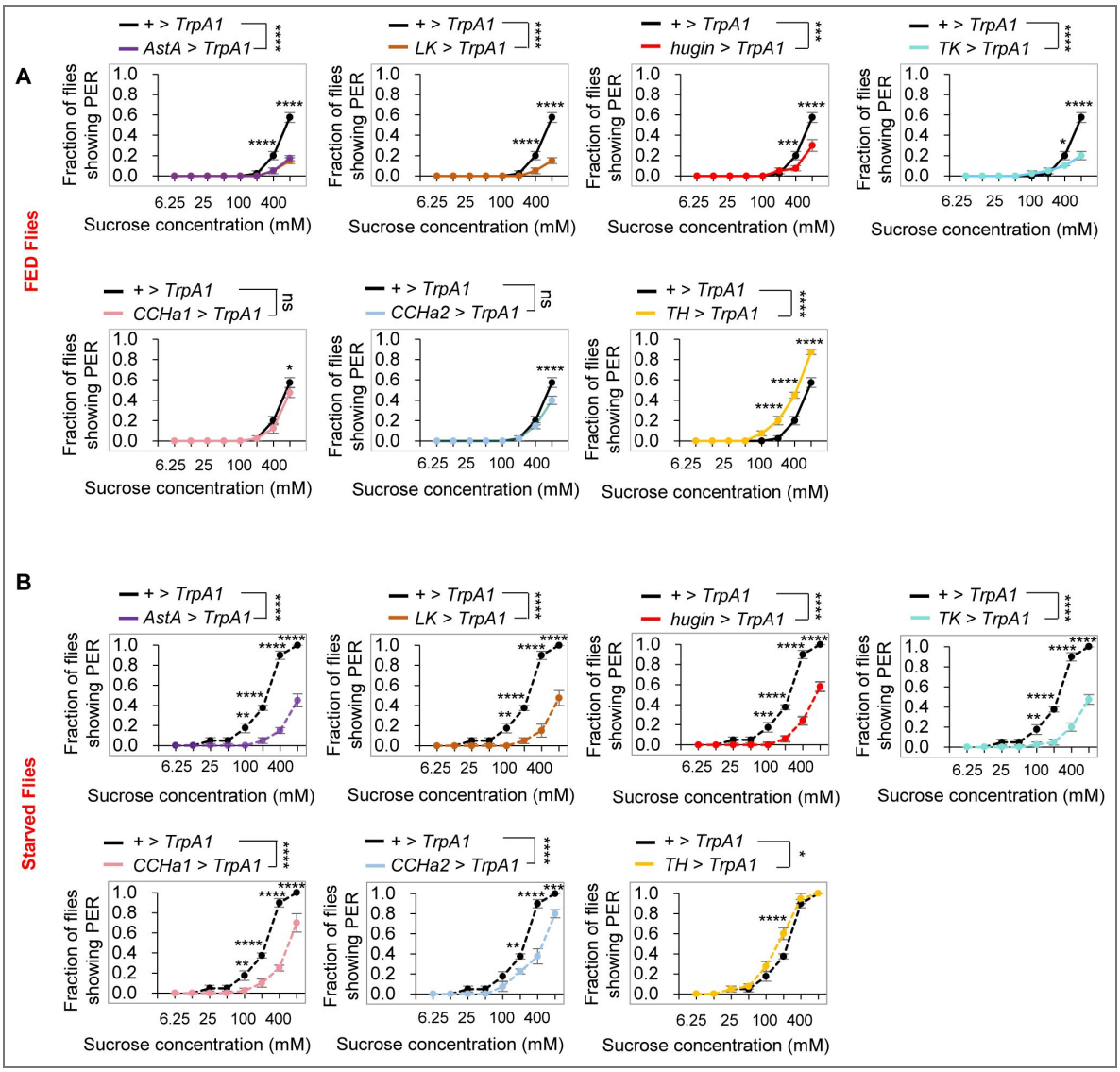

Figure supplementary 2. The effect of satiety signals on taste modulation.

(**A**) Fraction of fed flies of the indicated genotypes and environmental temperatures showing PER to different concentrations of sucrose (n=4 groups, each of 10 flies). (**B**) Fraction of starved flies of the indicated genotypes and environmental temperatures showing PER to different concentrations of sucrose (n=4-5 groups, each of 10 flies). ns, P > 0.05; *P < 0.05; ***P < 0.001; ****P < 0.0001. Two-way ANOVA followed by post hoc test with Bonferroni correction was used for multiple comparisons when applicable.

Figure supplementary 3. Activation of IPCs decreased the circulating sugar levels and increased sweet sensitivity.

(**A**) Hemolymph glucose levels from the indicated genotypes and treatment temperatures (n=8-9, 1 hour at 30 °C). (**B-C**) Fraction of fed flies of the indicated genotypes and environmental temperatures showing PER to different concentrations of sucrose (n=4 groups, each of 10 flies). ns, P > 0.05; ****P < 0.0001. Student's *t-test* and two-way ANOVA followed by post hoc test with Bonferroni correction were used for multiple comparisons when applicable.

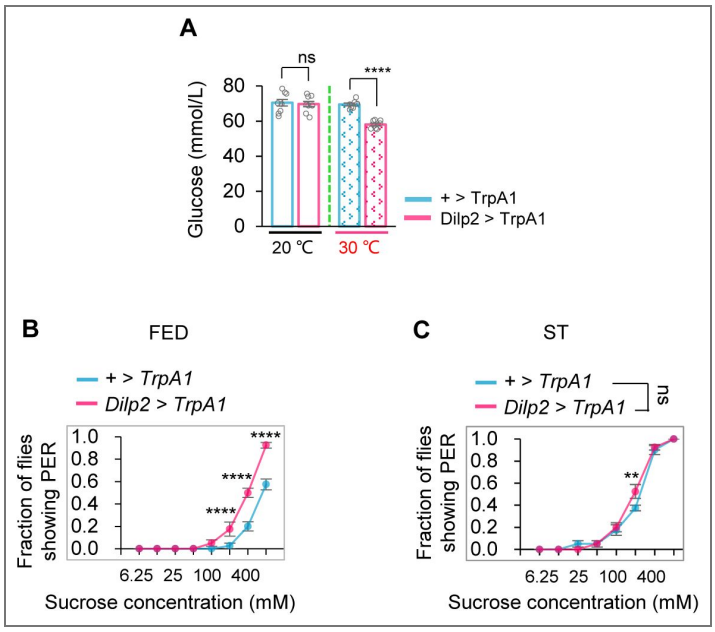

Figure supplementary 4. Sugar intake suppressed sweet sensation.

(**A**) Fraction of indicated flies showing PER to different concentrations of fructose (n=4 groups, each of 10 flies). (**B**) Fraction of indicated flies showing PER to different concentrations of trehalose (n=4 groups, each of 10 flies).****P < 0.0001. two-way ANOVA followed by post hoc test with Bonferroni correction were used for multiple comparisons when applicable.

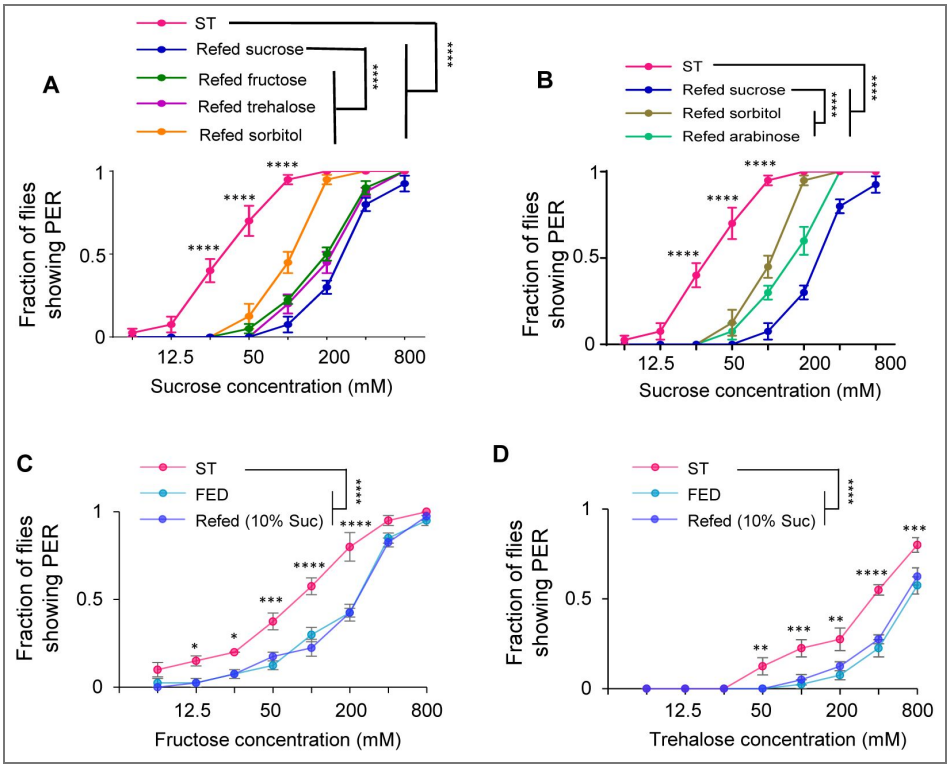

Figure supplementary 5. **Starvation led to a decrease in the circulating sugar levels.**

Hemolymph glucose levels from indicated flies (n=6-8). ***P < 0.001. Student's *t-test* was used for comparisons.

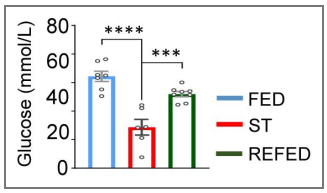

Figure supplementary 6. **The response of different neuropeptide-expressing neurons to glucose.**

(**A**) LK expression in the brain, illustrated by mCD8::GFP expression driven by LK^{GAL4}. Scale bar represents 100 μm. (**B**) Representative traces and quantification of ex vivo calcium responses of LK^{+} neurons during the perfusion of glucose (n=6). (**C-D**) The distribution (C) and calcium responses (D) of TK^{+} neurons (n=6). (**E-F**) The distribution (E) and calcium responses (F) of $CCHa1^{+}$ neurons (n=6). (**G-H**) The distribution (G) and calcium responses (H) of $CCHa2^{+}$ neurons (n=6).

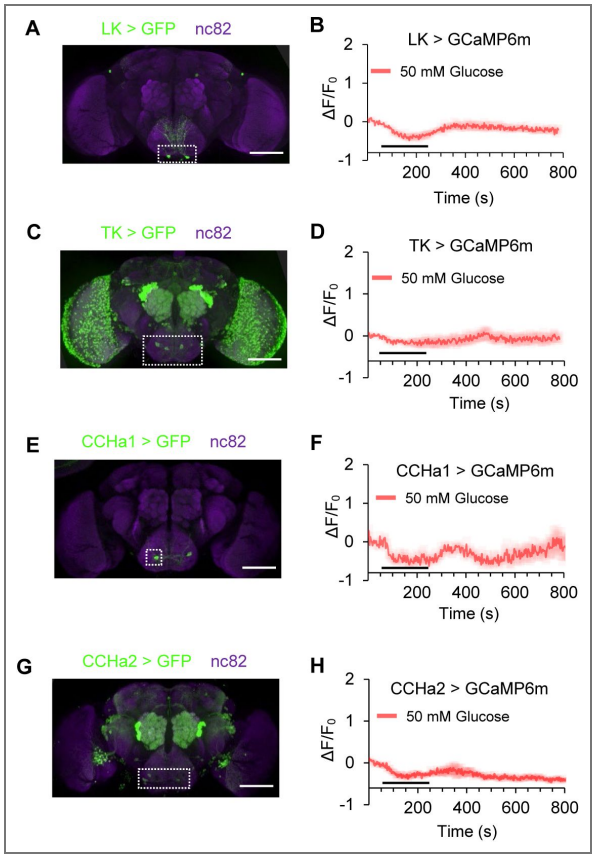

Figure supplementary 7. The calcium response of hugin neurons upon glucose stimuli.

(**A**) Representative image of hugin neurons in SEZ. Scale bar represents 50 μm. (**B**) Calcium responses of different cluster of hugin neurons during the prefusion of glucose (n=6)..*P < 0.05; ***P < 0.001. Student's *t-test* used for comparisons.

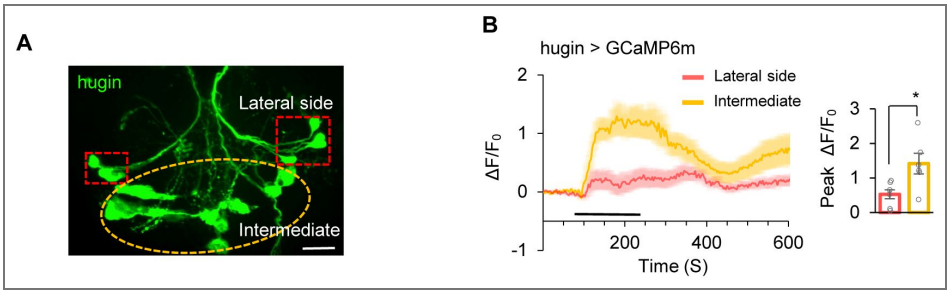

Figure supplementary 8. hugin^{+} or AstA^{+} neurons suppressed sweet taste.

(**A-D**) Fraction of flies of the indicated genotypes and environmental temperatures showing PER to different concentrations of sucrose (n=4-5 groups, each of 10 flies). ns, P > 0.05; *P < 0.05; ***P < 0.001; ****P < 0.0001. Two-way ANOVA followed by post hoc test with Bonferroni correction was used for multiple comparisons when applicable.

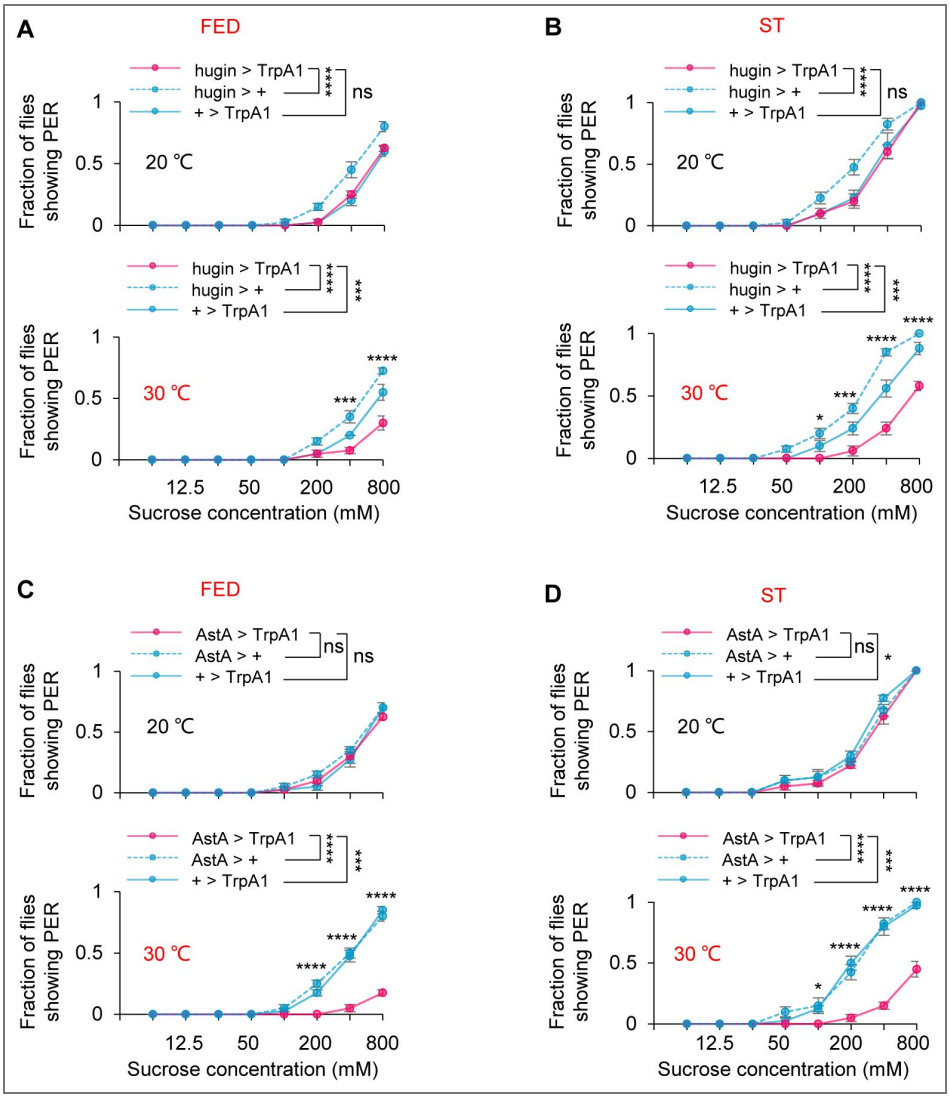

Figure supplementary 9. The calcium response of AstA^{+} neurons upon glucose treatment.

(**A**) Representative image of different part of AstA neurons. Scale bar represents 50 μm. (**B**) Calcium responses of different cluster of hugin neurons during the prefusion of glucose (n=6)

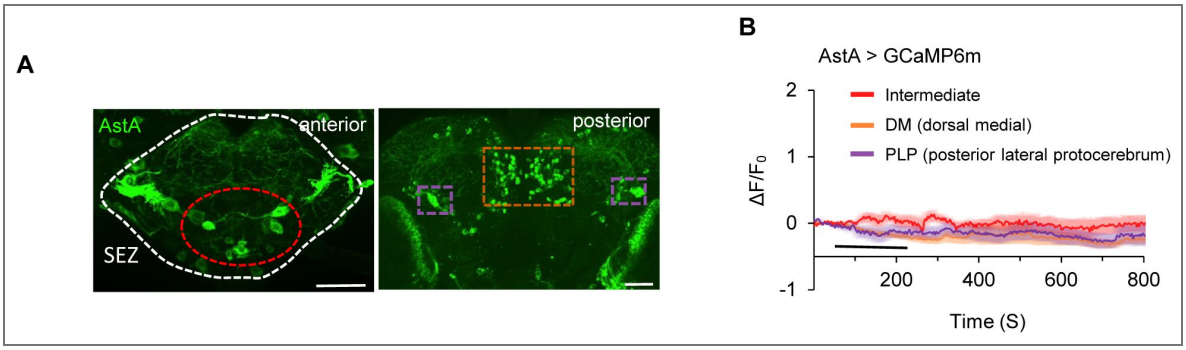

Figure supplementary 10. Knockout of *PK2-R1* enhanced sweet sensation.

(**A-C**) Fraction of flies of the indicated genotypes showing PER to different concentrations of sucrose (n=4 groups, each of 10 flies). ***P < 0.001; ****P < 0.0001. Two-way ANOVA followed by post hoc test with Bonferroni correction were used for multiple comparisons when applicable.

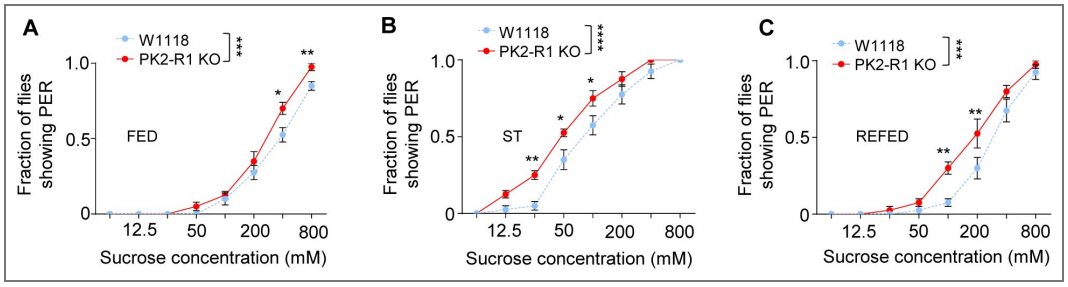

Figure supplementary 11. **hugin$^+$ neurons in the brain activated AstA$^+$ neurons.**

(**A-B**) Fraction of flies of the indicated genotypes and environmental temperatures showing PER to different concentrations of sucrose (n=4 groups, each of 10 flies). Note connection between the brain and VNC was cut off before the behavioral assay. (**C**) Representative traces (upper) and quantification (lower) of peak calcium transients of AstA$^+$ neurons after the photo-activation of hugin$^+$ neurons (n=6) from ex vivo calcium imaging. Horizontal black bar represents the duration of red-light stimulation.

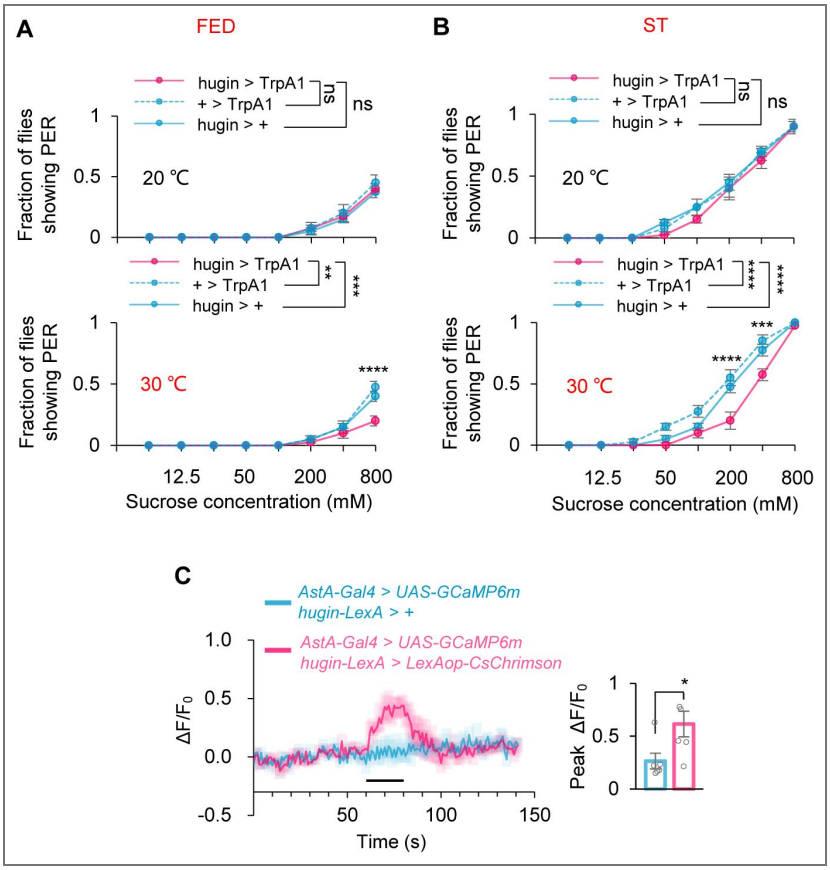

Figure supplementary 12. **Manipulating gene *AstA-R1* enhance PER.**

(**A-C**) Fraction of flies of the indicated genotypes showing PER to different concentrations of sucrose (n=4 groups, each of 10 flies). ***P < 0.001; ****P < 0.0001. Two-way ANOVA followed by post hoc test with Bonferroni correction were used for multiple comparisons when applicable.

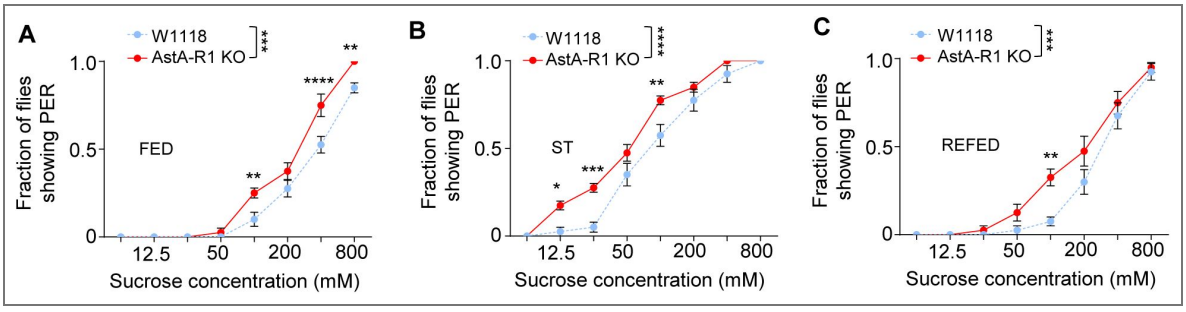

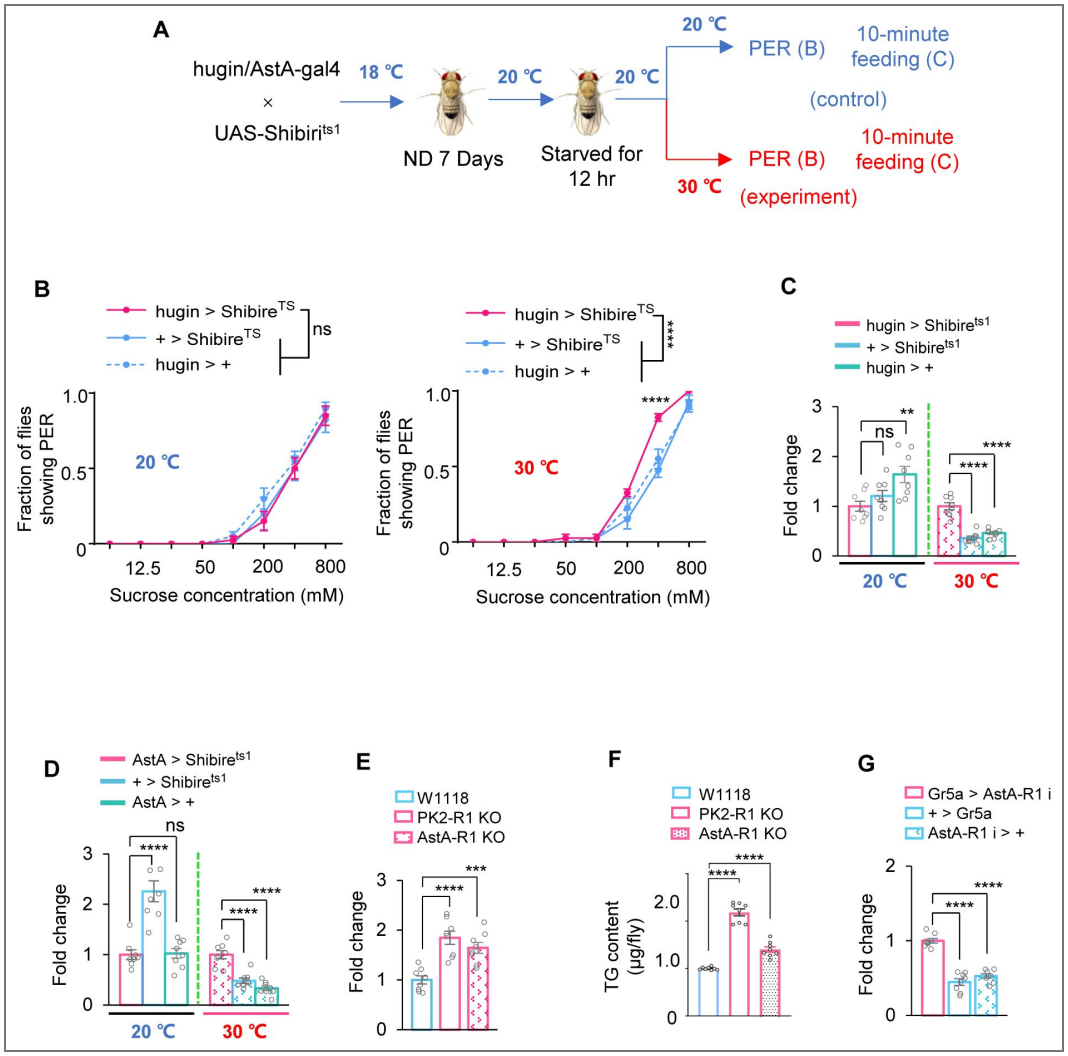

Figure supplementary 13. hugin-AstA-Gr5a circuitry inhibited feeding behavior.

(**A**) The illustration of experimental design in Figure supplementary 13B-C. Note that all flies were maintained at 20°C before the feeding assay to prevent neuronal silencing by Shibire^{ts1} during these procedures. (B) Fraction of flies of the indicated genotypes and environmental temperatures showing PER to different concentrations of sucrose (n=4 groups, each of 10 flies). (**C-D**) Food consumption of flies of the indicated genotypes and environmental temperatures (n=8 groups, each of 4 flies). Food consumption is presented as fold change relative to the corresponding genetic control. (**E**) Food consumption of flies of the indicated genotypes (n=8 groups, each of 4 flies). (**F**) The TG content of indicated genotypes (n=8 groups, each of 2 flies). (**G**) Food consumption of flies of the indicated genotypes (n=8 groups, each of 4 flies). ns, P > 0.05; ***P < 0.001; ****P < 0.0001. Student's *t-test* and two-way ANOVA followed by post hoc test with Bonferroni correction were used for multiple comparisons when applicable.

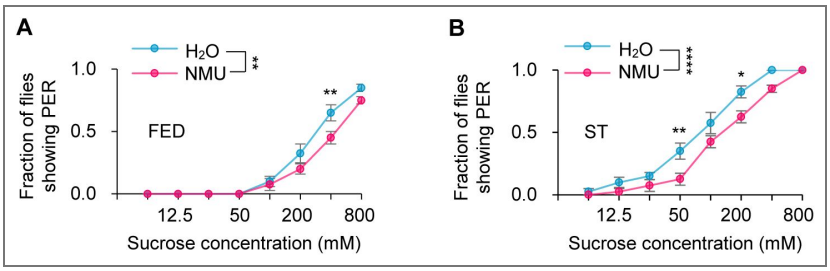

Figure supplementary 14. NMU peptide suppressed sweet taste in fly.

Fraction of flies showing PER to different concentrations of sucrose (n=4 groups, each of 10 flies). Flies were injected with saline or synthetic NMU for 30 mins before the assay.**P < 0.01; ****P < 0.0001. Two-way ANOVA followed by post hoc test with Bonferroni correction were used for multiple comparisons when applicable.

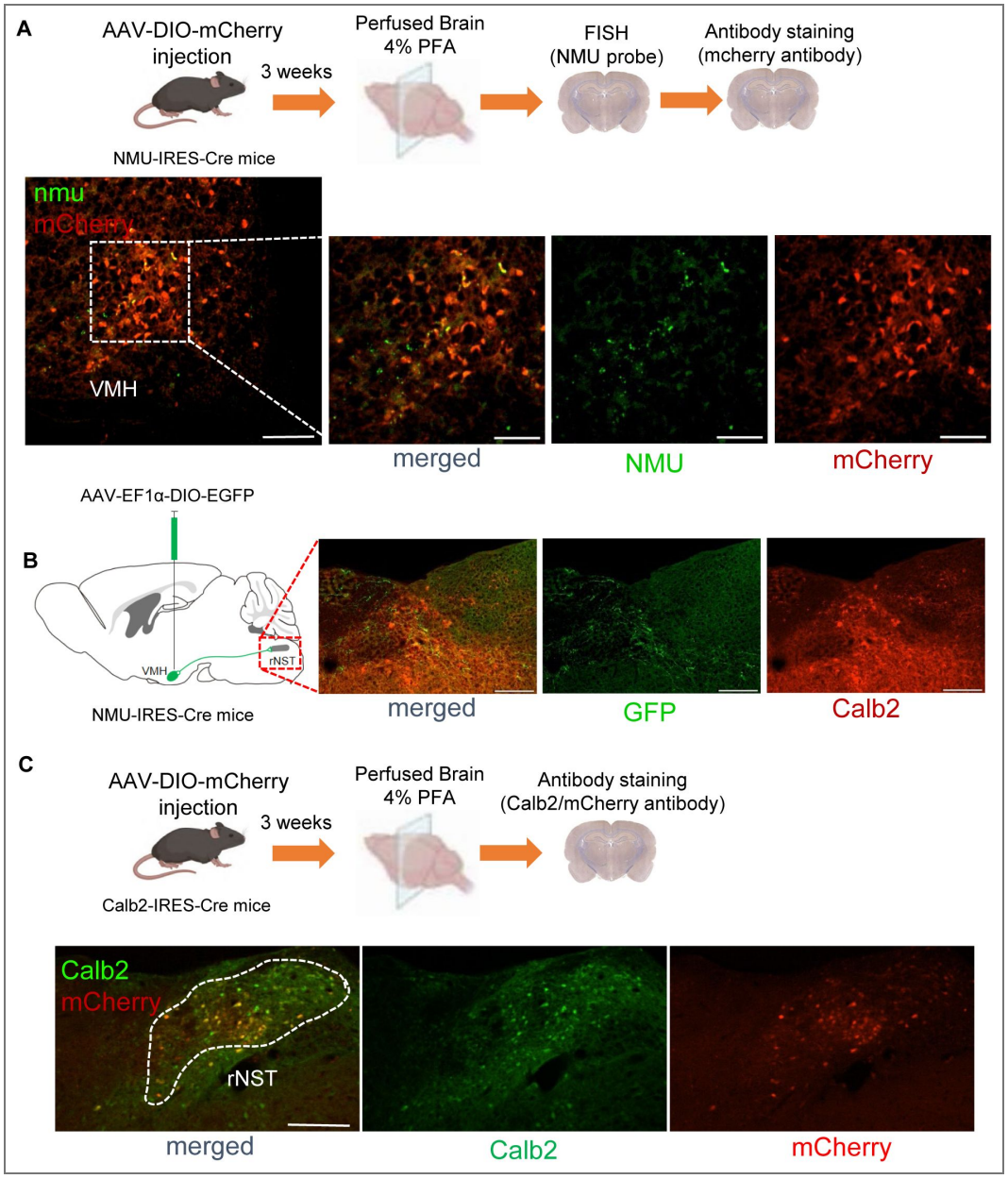

Figure supplementary 15. The expressing pattern of NMU neurons and Calb2 neurons

(**A**) Co-labeling of NMU^{+} neurons using a Cre-dependent mCherry reporter (red) and in situ hybridization (green).Scale bar represents 200 μm. (**B**) NMU arbors was extended near Calb2^{rNST} neurons. Scale bar represents 200 μm. (**C**) Co-labeling of Calb2^{+} neurons with a Cre-dependent mCherry reporter (red) and NMU antiboy staining (green). Scale bar represents 200 μm.

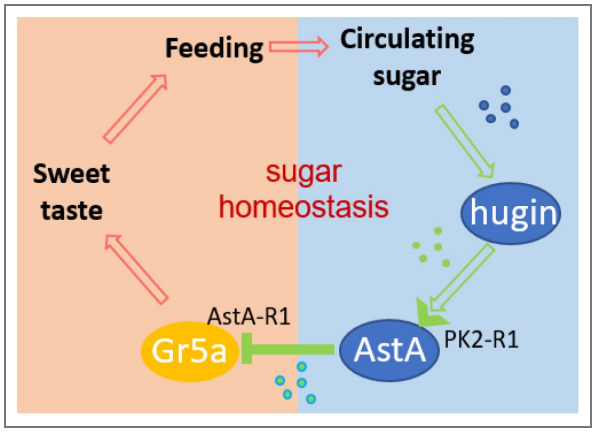

Figure supplementary 16. **A working model**

In the fly brain, a small group of neurons expressing hugin peptide is responsible for detecting the circulating glucose levels. Following feeding, as the levels of glucose in the circulatory system increased, these neurons are activated, leading to the release of hugin, which activated AstA neurons via its receptor PK2-R1. Subsequently, the activation of $AstA^{+}$ neurons then directly inhibited sweet perception via AstA peptide and its cognate receptor AstA-R1 expressed in sweet-sensing $Gr5a^{+}$ neurons. This neural circuitry is a novel energy sensor that suppressed sweet perception and terminated feeding behavior, providing an efficient mechanism for maintaining energy homeostasis.

Data availability

Source data contain the numerical data used to generate the figures.

Acknowledgements

We express gratitude to all members of the Wang and Huang Lab for their valuable discussions and technical support. Special thanks to Yi Rao and Bowen Deng for generously providing *Drosophila* chemoconnectome lines, and to Yulong Li and Jianzhi Zeng for their assistance with *in vivo* calcium imaging preparations. Appreciation is extended to the members of the Neuroscience Pioneer Club for their insightful discussions throughout the course of this study. This study was funded by the National Natural Science Foundation of China (No. 32071006 for L.W. and No. 32271008 for R.H.), Guangdong Basic and Applied Basic Research Foundation (2023A1515110454 for T.S.), and the startup funds from Shenzhen Bay Laboratory and Chinese Institutes for Medical Research to L.W.

Additional information

Author contributions

T.S., R.H., and L.W. designed the experiments and wrote the manuscript. W.Q., and T.S. conducted and analyzed all the experiments. L.W. and R.H. supervised the project.

Funding

Funder	Grant reference number	Author
MOST | National Natural Science Foundation of China (NSFC)	32271008	Rui Huang
MOST | National Natural Science Foundation of China (NSFC)	32071006	Liming Wang
Guangdong Basic and Applied Basic Research Foundation	2023A1515110454	Tingting Song

Author ORCID iDs

Liming Wang: https://orcid.org/0000-0002-7256-8776

Additional files

Sourc data 1. Source data for all figures.

References

1. **Ritterhoff J.,** Tian R (2023) Metabolic mechanisms in physiological and pathological cardiac hypertrophy: new paradigms and challenges. *Nat Rev Cardiol* **20**:812-829 https://doi.org/10.1038/s41569-023-00887-x
2. **Smith N.K.,** Plotkin J.M., Grueter B.A (2022) Hunger dampens a nucleus accumbens circuit to drive persistent food seeking. *Curr Biol* **32**:1689-1702 e1684 https://doi.org/10.1016/j.cub.2022.02.034
3. **Yu Y.,** Huang R., Ye J., Zhang V., Wu C., Cheng G., Jia J., Wang L (2016) Regulation of starvation-induced hyperactivity by insulin and glucagon signaling in adult Drosophila. *eLife* **5** https://doi.org/10.7554/eLife.15693
4. **Roh E.,** Kim M.S (2016) Brain Regulation of Energy Metabolism. *Endocrinol Metab (Seoul)* **31**:519-524 https://doi.org/10.3803/EnM.2016.31.4.519

5. **Tan H.L.,** Yin L., Tan Y., Ivanov J., Plucinska K., Ilanges A., Herb B.R., Wang P., Kosse C., Cohen P., *et al.* (2024) Leptin-activated hypothalamic BNC2 neurons acutely suppress food intake. *Nature* **636**:198-205 https://doi.org/10.1038/s41586-024-08108-2
6. **De Solis A.J.,** Del Rio-Martin A., Radermacher J., Chen W., Steuernagel L., Bauder C.A., Eggersmann F.R., Morgan D.A., Cremer A.L., Sue M., *et al.* (2024) Reciprocal activity of AgRP and POMC neurons governs coordinated control of feeding and metabolism. *Nat Metab* **6**:473-493 https://doi.org/10.1038/s42255-024-00987-z
7. **Sayar-Atasoy N.,** Aklan I., Yavuz Y., Laule C., Kim H., Rysted J., Alp M.I., Davis D., Yilmaz B., Atasoy D (2024) AgRP neurons encode circadian feeding time. *Nat Neurosci* **27**:102-115 https://doi.org/10.1038/s41593-023-01482-6
8. **Chung B.Y.,** Ro J., Hutter S.A., Miller K.M., Guduguntla L.S., Kondo S., Pletcher S.D (2017) Drosophila Neuropeptide F Signaling Independently Regulates Feeding and Sleep-Wake Behavior. *Cell Rep* **19**:2441-2450 https://doi.org/10.1016/j.celrep.2017.05.085
9. **Shohat-Ophir G.,** Kaun K.R., Azanchi R., Mohammed H., Heberlein U (2012) Sexual deprivation increases ethanol intake in Drosophila. *Science* **335**:1351-1355 https://doi.org/10.1126/science.1215932
10. **Inagaki H.K.,** Ben-Tabou de-Leon S., Wong A.M., Jagadish S., Ishimoto H., Barnea G., Kitamoto T., Axel R., Anderson D.J (2012) Visualizing neuromodulation in vivo: TANGO-mapping of dopamine signaling reveals appetite control of sugar sensing. *Cell* **148**:583-595 https://doi.org/10.1016/j.cell.2011.12.022
11. **Qi W.,** Wang G., Wang L (2021) A novel satiety sensor detects circulating glucose and suppresses food consumption via insulin-producing cells in Drosophila. *Cell Res* **31**:580-588 https://doi.org/10.1038/s41422-020-00449-7
12. **Zhao Y.,** Khallaf M.A., Johansson E., Dzaki N., Bhat S., Alfredsson J., Duan J., Hansson B.S., Knaden M., Alenius M (2022) Hedgehog-mediated gut-taste neuron axis controls sweet perception in Drosophila. *Nat Commun* **13** https://doi.org/10.1038/s41467-022-35527-4
13. **Oh Y.,** Lai J.S., Mills H.J., Erdjument-Bromage H., Giammarinaro B., Saadipour K., Wang J.G., Abu F., Neubert T.A., Suh G.S.B (2019) A glucose-sensing neuron pair regulates insulin and glucagon in Drosophila. *Nature* **574**:559-564 https://doi.org/10.1038/s41586-019-1675-4
14. **Dus M.,** Lai J.S., Gunapala K.M., Min S., Tayler T.D., Hergarden A.C., Geraud E., Joseph C.M., Suh G.S (2015) Nutrient Sensor in the Brain Directs the Action of the Brain-Gut Axis in Drosophila. *Neuron* **87**:139-151 https://doi.org/10.1016/j.neuron.2015.05.032
15. **Schlegel P.,** Texada M.J., Miroschnikow A., Schoofs A., Huckesfeld S., Peters M., Schneider-Mizell C.M., Lacin H., Li F., Fetter R.D., *et al.* (2016) Synaptic transmission parallels neuromodulation in a central food-intake circuit. *eLife* **5** https://doi.org/10.7554/eLife.16799
16. **Schoofs A.,** Huckesfeld S., Schlegel P., Miroschnikow A., Peters M., Zeymer M., Spiess R., Chiang A.S., Pankratz M.J (2014) Selection of motor programs for suppressing food intake and inducing locomotion in the Drosophila brain. *PLoS Biol* **12**:e1001893 https://doi.org/10.1371/journal.pbio.1001893
17. **Hergarden A.C.,** Tayler T.D., Anderson D.J (2012) Allatostatin-A neurons inhibit feeding behavior in adult Drosophila. *Proc Natl Acad Sci U S A* **109**:3967-3972 https://doi.org/10.1073/pnas.1200778109
18. **Melcher C.,** Bader R., Walther S., Simakov O., Pankratz M.J (2006) Neuromedin U and its putative Drosophila homolog hugin. *PLoS Biol* **4**:e68 https://doi.org/10.1371/journal.pbio.0040068
19. **Munch D.,** Ezra-Nevo G., Francisco A.P., Tastekin I., Ribeiro C (2020) Nutrient homeostasis - translating internal states to behavior. *Curr Opin Neurobiol* **60**:67-75 https://doi.org/10.1016/j.conb.2019.10.004
20. **Marella S.,** Mann K., Scott K (2012) Dopaminergic modulation of sucrose acceptance behavior in Drosophila. *Neuron* **73**:941-950 https://doi.org/10.1016/j.neuron.2011.12.032
21. **Augustine V.,** Lee S., Oka Y (2020) Neural Control and Modulation of Thirst, Sodium Appetite, and Hunger. *Cell* **180**:25-32 https://doi.org/10.1016/j.cell.2019.11.040

22. **de Rivaz R.,** Swendsen J., Berthoz S., Husky M., Merikangas K., Marques-Vidal P. (2022) Associations between Hunger and Psychological Outcomes: A Large-Scale Ecological Momentary Assessment Study. *Nutrients* **14** https://doi.org/10.3390/nu14235167

23. **Alhadeff A.L.,** Su Z., Hernandez E., Klima M.L., Phillips S.Z., Holland R.A., Guo C., Hantman A.W., De Jonghe B.C., Betley J.N. (2018) A Neural Circuit for the Suppression of Pain by a Competing Need State. *Cell* **173**:140-152 e115 https://doi.org/10.1016/j.cell.2018.02.057

24. **Sun M.,** Ma M., Deng B., Li N., Peng Q., Pan Y (2023) A neural pathway underlying hunger modulation of sexual receptivity in Drosophila females. *Cell Rep* **42** https://doi.org/10.1016/j.celrep.2023.113243

25. **Burnett C.J.,** Li C., Webber E., Tsaousidou E., Xue S.Y., Bruning J.C., Krashes M.J (2016) Hunger-Driven Motivational State Competition. *Neuron* **92**:187-201 https://doi.org/10.1016/j.neuron.2016.08.032

26. **Deem J.D.,** Faber C.L., Morton G.J (2022) AgRP neurons: Regulators of feeding, energy expenditure, and behavior. *Febs J* **289**:2362-2381 https://doi.org/10.1111/febs.16176

27. **Karigo T.,** Deutsch D (2022) Flexibility of neural circuits regulating mating behaviors in mice and flies. *Front Neural Circuits* **16** https://doi.org/10.3389/fncir.2022.949781

28. **Fu O.,** Iwai Y., Narukawa M., Ishikawa A.W., Ishii K.K., Murata K., Yoshimura Y., Touhara K., Misaka T., Minokoshi Y., *et al.* (2019) Hypothalamic neuronal circuits regulating hunger-induced taste modification. *Nat Commun* **10** https://doi.org/10.1038/s41467-019-12478-x

29. **Dietrich M.O.,** Zimmer M.R., Bober J., Horvath T.L (2015) Hypothalamic Agrp neurons drive stereotypic behaviors beyond feeding. *Cell* **160**:1222-1232 https://doi.org/10.1016/j.cell.2015.02.024

30. **Bruning J.C.,** Fenselau H (2023) Integrative neurocircuits that control metabolism and food intake. *Science* **381**:eabl7398 https://doi.org/10.1126/science.abl7398

31. **Chen Y.,** Lin Y.C., Kuo T.W., Knight Z.A (2015) Sensory detection of food rapidly modulates arcuate feeding circuits. *Cell* **160**:829-841 https://doi.org/10.1016/j.cell.2015.01.033

32. **Koch M.,** Varela L., Kim J.G., Kim J.D., Hernandez-Nuno F., Simonds S.E., Castorena C.M., Vianna C.R., Elmquist J.K., Morozov Y.M., *et al.* (2015) Hypothalamic POMC neurons promote cannabinoid-induced feeding. *Nature* **519**:45-50 https://doi.org/10.1038/nature14260

33. **Belgardt B.F.,** Okamura T., Bruning J.C (2009) Hormone and glucose signalling in POMC and AgRP neurons. *J Physiol* **587**:5305-5314 https://doi.org/10.1113/jphysiol.2009.179192

34. **Vivot K.,** Meszaros G., Pangou E., Zhang Z., Qu M., Erbs E., Yeghiazaryan G., Quinones M., Grandgirard E., Schneider A., *et al.* (2023) CaMK1D signalling in AgRP neurons promotes ghrelin-mediated food intake. *Nat Metab* **5**:1045-1058 https://doi.org/10.1038/s42255-023-00814-x

35. **Wei Q.,** Krolewski D.M., Moore S., Kumar V., Li F., Martin B., Tomer R., Murphy G.G., Deisseroth K., Watson S.J., *et al.* (2018) Uneven balance of power between hypothalamic peptidergic neurons in the control of feeding. *Proc Natl Acad Sci U S A* **115**:E9489-E9498 https://doi.org/10.1073/pnas.1802237115

36. **Lin S.,** Senapati B., Tsao C.H (2019) Neural basis of hunger-driven behaviour in Drosophila. *Open Biol* **9** https://doi.org/10.1098/rsob.180259

37. **Chouhan N.S.,** Griffith L.C., Haynes P., Sehgal A (2021) Availability of food determines the need for sleep in memory consolidation. *Nature* **589**:582-585 https://doi.org/10.1038/s41586-020-2997-y

38. **Willyard C** (2008) Hungry for sleep. *Nat Med* **14**:477-480 https://doi.org/10.1038/nm0508-477

39. **Yao Z.,** Scott K (2022) Serotonergic neurons translate taste detection into internal nutrient regulation. *Neuron* **110**:1036-1050 e1037 https://doi.org/10.1016/j.neuron.2021.12.028

40. **Malita A.,** Kubrak O., Koyama T., Ahrentlov N., Texada M.J., Nagy S., Halberg K.V., Rewitz K (2022) A gut-derived hormone suppresses sugar appetite and regulates food choice in Drosophila. *Nat Metab* **4**:1532-1550 https://doi.org/10.1038/s42255-022-00672-z

41. **Melcher C.,** Pankratz M.J (2005) Candidate gustatory interneurons modulating feeding behavior in the Drosophila brain. *PLoS Biol* **3**:e305 https://doi.org/10.1371/journal.pbio.0030305

42. **Root C.M.,** Ko K.I., Jafari A., Wang J.W (2011) Presynaptic facilitation by neuropeptide signaling mediates odor-driven food search. *Cell* **145**:133-144 https://doi.org/10.1016/j.cell.2011.02.008

43. **Chen J.,** Reiher W., Hermann-Luibl C., Sellami A., Cognigni P., Kondo S., Helfrich-Forster C., Veenstra J.A., Wegener C (2016) Allatostatin A Signalling in Drosophila Regulates Feeding and Sleep and Is Modulated by PDF. *PLoS Genet* **12**:e1006346 https://doi.org/10.1371/journal.pgen.1006346

44. **Hentze J.L.,** Carlsson M.A., Kondo S., Nassel D.R., Rewitz K.F (2015) The Neuropeptide Allatostatin A Regulates Metabolism and Feeding Decisions in Drosophila. *Sci Rep* **5** https://doi.org/10.1038/srep11680

45. **Kubrak O.I.,** Lushchak O.V., Zandawala M., Nassel D.R (2016) Systemic corazonin signalling modulates stress responses and metabolism in Drosophila. *Open Biol* **6** https://doi.org/10.1098/rsob.160152

46. **Martelli C.,** Pech U., Kobbenbring S., Pauls D., Bahl B., Sommer M.V., Pooryasin A., Barth J., Arias C.W.P., Vassiliou C., *et al.* (2017) SIFamide Translates Hunger Signals into Appetitive and Feeding Behavior in Drosophila. *Cell Rep* **20**:464-478 https://doi.org/10.1016/j.celrep.2017.06.043

47. **Ugrankar R.,** Theodoropoulos P., Akdemir F., Henne W.M., Graff J.M (2018) Circulating glucose levels inversely correlate with Drosophila larval feeding through insulin signaling and SLC5A11. *Commun Biol* **1** https://doi.org/10.1038/s42003-018-0109-4

48. **Oh Y.,** Lai J.S., Min S., Huang H.W., Liberles S.D., Ryoo H.D., Suh G.S.B (2021) Periphery signals generated by Piezo-mediated stomach stretch and Neuromedin-mediated glucose load regulate the Drosophila brain nutrient sensor. *Neuron* **109**:1979-1995 e1976 https://doi.org/10.1016/j.neuron.2021.04.028

49. **Senapati B.,** Tsao C.H., Juan Y.A., Chiu T.H., Wu C.L., Waddell S., Lin S (2019) A neural mechanism for deprivation state-specific expression of relevant memories in Drosophila. *Nat Neurosci* **22**:2029-2039 https://doi.org/10.1038/s41593-019-0515-z

50. **Yurgel M.E.,** Kakad P., Zandawala M., Nassel D.R., Godenschwege T.A., Keene A.C (2019) A single pair of leucokinin neurons are modulated by feeding state and regulate sleep-metabolism interactions. *PLoS Biol* **17**:e2006409 https://doi.org/10.1371/journal.pbio.2006409

51. **Song T.,** Qin W., Lai Z., Li H., Li D., Wang B., Deng W., Wang T., Wang L., Huang R (2023) Dietary cysteine drives body fat loss via FMRFamide signaling in Drosophila and mouse. *Cell Res* **33**:434-447 https://doi.org/10.1038/s41422-023-00800-8

52. **Inagaki H.K.,** Panse K.M., Anderson D.J (2014) Independent, reciprocal neuromodulatory control of sweet and bitter taste sensitivity during starvation in Drosophila. *Neuron* **84**:806-820 https://doi.org/10.1016/j.neuron.2014.09.032

53. **Fujii S.,** Yavuz A., Slone J., Jagge C., Song X., Amrein H (2015) Drosophila sugar receptors in sweet taste perception, olfaction, and internal nutrient sensing. *Curr Biol* **25**:621-627 https://doi.org/10.1016/j.cub.2014.12.058

54. **Budnik V.,** White K (1987) Genetic dissection of dopamine and serotonin synthesis in the nervous system of Drosophila melanogaster. *J Neurogenet* **4**:309-314

55. **Deng B.,** Li Q., Liu X., Cao Y., Li B., Qian Y., Xu R., Mao R., Zhou E., Zhang W., *et al.* (2019) Chemoconnectomics: Mapping Chemical Transmission in Drosophila. *Neuron* **101**:876-893 e874 https://doi.org/10.1016/j.neuron.2019.01.045

56. **Yoon N.A.,** Diano S (2021) Hypothalamic glucose-sensing mechanisms. *Diabetologia* **64**:985-993 https://doi.org/10.1007/s00125-021-05395-6

57. **Brogiolo W.,** Stocker H., Ikeya T., Rintelen F., Fernandez R., Hafen E (2001) An evolutionarily conserved function of the Drosophila insulin receptor and insulin-like peptides in growth control. *Curr Biol* **11**:213-221 https://doi.org/10.1016/s0960-9822(01)00068-9

58. **Fosque B.F.,** Sun Y., Dana H., Yang C.T., Ohyama T., Tadross M.R., Patel R., Zlatic M., Kim D.S., Ahrens M.B., *et al.* (2015) Neural circuits. Labeling of active neural circuits in vivo with designed calcium integrators. *Science* **347**:755-760 https://doi.org/10.1126/science.1260922

59. **Parton L.E.,** Ye C.P., Coppari R., Enriori P.J., Choi B., Zhang C.Y., Xu C., Vianna C.R., Balthasar N., Lee C.E., *et al.* (2007) Glucose sensing by POMC neurons regulates glucose homeostasis and is impaired in obesity. *Nature* **449**:228-232 https://doi.org/10.1038/nature06098

60. **Wang M.,** Wu J.X., Ding D., Chen L (2022) Structural insights into the mechanism of pancreatic K(ATP) channel regulation by nucleotides. *Nat Commun* **13** https://doi.org/10.1038/s41467-022-30430-4

61. **Park Y.,** Kim Y.J., Adams M.E (2002) Identification of G protein-coupled receptors for Drosophila PRXamide peptides, CCAP, corazonin, and AKH supports a theory of ligand-receptor coevolution. *Proc Natl Acad Sci U S A* **99**:11423-11428 https://doi.org/10.1073/pnas.162276199

62. **Klapoetke N.C.,** Murata Y., Kim S.S., Pulver S.R., Birdsey-Benson A., Cho Y.K., Morimoto T.K., Chuong A.S., Carpenter E.J., Tian Z., *et al.* (2014) Independent optical excitation of distinct neural populations. *Nat Methods* **11**:338-346 https://doi.org/10.1038/nmeth.2836

63. **Dahanukar A.,** Lei Y.T., Kwon J.Y., Carlson J.R (2007) Two Gr genes underlie sugar reception in Drosophila. *Neuron* **56**:503-516 https://doi.org/10.1016/j.neuron.2007.10.024

64. **Larsen M.J.,** Burton K.J., Zantello M.R., Smith V.G., Lowery D.L., Kubiak T.M (2001) Type A allatostatins from Drosophila melanogaster and Diplotera puncata activate two Drosophila allatostatin receptors, DAR-1 and DAR-2, expressed in CHO cells. *Biochem Biophys Res Commun* **286**:895-901 https://doi.org/10.1006/bbrc.2001.5476

65. **Kitamoto T** (2001) Conditional modification of behavior in Drosophila by targeted expression of a temperature-sensitive shibire allele in defined neurons. *J Neurobiol* **47**:81-92 https://doi.org/10.1002/neu.1018

66. **Stocker R.F** (2004) Taste perception: Drosophila - a model of good taste. *Curr Biol* **14**:R560-561 https://doi.org/10.1016/j.cub.2004.07.011

67. **Yarmolinsky D.A.,** Zuker C.S., Ryba N.J (2009) Common sense about taste: from mammals to insects. *Cell* **139**:234-244 https://doi.org/10.1016/j.cell.2009.10.001

68. **Jin H.,** Fishman Z.H., Ye M., Wang L., Zuker C.S (2021) Top-Down Control of Sweet and Bitter Taste in the Mammalian Brain. *Cell* **184**:257-271 e216 https://doi.org/10.1016/j.cell.2020.12.014

69. **Kain P.,** Dahanukar A (2015) Secondary taste neurons that convey sweet taste and starvation in the Drosophila brain. *Neuron* **85**:819-832 https://doi.org/10.1016/j.neuron.2015.01.005

70. **Williams M.J.,** Akram M., Barkauskaite D., Patil S., Kotsidou E., Kheder S., Vitale G., Filaferro M., Blemings S.W., Maestri G., *et al.* (2020) CCAP regulates feeding behavior via the NPF pathway in Drosophila adults. *Proc Natl Acad Sci U S A* **117**:7401-7408 https://doi.org/10.1073/pnas.1914037117

71. **Matsushita R.,** Nishimura T (2020) Trehalose metabolism confers developmental robustness and stability in Drosophila by regulating glucose homeostasis. *Commun Biol* **3** https://doi.org/10.1038/s42003-020-0889-1

72. **Ma D.,** Hu M., Yang X., Liu Q., Ye F., Cai W., Wang Y., Xu X., Chang S., Wang R., *et al.* (2024) Structural basis for sugar perception by Drosophila gustatory receptors. *Science* **383**:eadj2609 https://doi.org/10.1126/science.adj2609

73. **Hanada R.,** Teranishi H., Pearson J.T., Kurokawa M., Hosoda H., Fukushima N., Fukue Y., Serino R., Fujihara H., Ueta Y., *et al.* (2004) Neuromedin U has a novel anorexigenic effect independent of the leptin signaling pathway. *Nat Med* **10**:1067-1073 https://doi.org/10.1038/nm1106

74. **Howard A.D.,** Wang R., Pong S.S., Mellin T.N., Strack A., Guan X.M., Zeng Z., Williams D.L., Feighner S.D., Nunes C.N., *et al.* (2000) Identification of receptors for neuromedin U and its role in feeding. *Nature* **406**:70-74 https://doi.org/10.1038/35017610

75. **Miroschnikow A.,** Schlegel P., Pankratz M.J (2020) Making Feeding Decisions in the Drosophila Nervous System. *Curr Biol* **30**:R831-R840 https://doi.org/10.1016/j.cub.2020.06.036

76. **Teranishi H.,** Hanada R (2021) Neuromedin U, a Key Molecule in Metabolic Disorders. *Int J Mol Sci* **22** https://doi.org/10.3390/ijms22084238

77. **Aldawsari M.,** Almadani F.A., Almuhammadi N., Algabsani S., Alamro Y., Aldhwayan M (2023) The Efficacy of GLP-1 Analogues on Appetite Parameters, Gastric Emptying, Food Preference and Taste Among Adults with Obesity: Systematic Review of Randomized Controlled Trials. *Diabetes Metab Syndr Obes* **16**:575-595 https://doi.org/10.2147/DMSO.S387116

78. **Sun J.,** Liu C., Bai X., Li X., Li J., Zhang Z., Zhang Y., Guo J., Li Y (2017) Drosophila FIT is a protein-specific satiety hormone essential for feeding control. *Nat Commun* **8** https://doi.org/10.1038/ncomms14161

Peer reviews

Reviewer #1 (Public review):

In this revised manuscript, Qin and colleagues aim to delineate a neural mechanism that is engaged specifically in the sated flies to suppress the intake of sugar solution (the "brake" mechanism for sugar consumption). They identified a three-step neuropeptidergic system that downregulates the sensitivity of sweet-sensing gustatory sensory neurons in sated flies. First, neurons that release a neuropeptide Hugin (which is an insect homolog of vertebrate Neuromedin U (NMU)) are in active state when the concentration of glucose is high. This activation depends on the cell-autonomous function of Hugin-releasing neurons that sense hemolymph glucose levels directly. Next, the Hugin neuropeptides activate Allatostatin A (AstA)-releasing neurons via one of Hugin receptors, PK2-R1. Finally, the released AstA neuropeptide suppresses sugar response in sugar-sensing Gr5a-expressing gustatory sensory neurons through AstA-R1 receptor. Suppression of sugar response in Gr5a-expressing neurons reduces fly's sugar intake motivation. They also found that NMU-expressing neurons in the ventromedial hypothalamus (VMH) of mice (which project to the rostal nucleus of the solitary tract (rNST)) are also activated by high concentrations of glucose independent of synaptic transmission, and that injection of NMU reduces the glucose-induced activity in the downstream of NMU-expressing neurons in rNST. These data suggest that the function of Hugin neuropeptide in the fly is analogous to the function of NMU in the mouse.

The shift of the narrative, which focuses specifically on the hugin-AstA axis as the "brake" on the satiety signal and feeding behavior, clarified the central message of the presented work. The authors have provided multiple lines of compelling evidence generated through rigorous experiments. The parallel study in mice adds a unique comparative perspective that makes the paper interesting to a wide range of readers.

While I deeply appreciate the authors' efforts to substantially restructure the manuscript, I have a few suggestions for further improvements. First, there remains room for discussion whether the "brake" function of the hugin-AstA axis is truly satiety state-dependent. The fact that neural activation (Fig. Supp. 8), peptide injection (Fig. 3A, 4A), receptor knockdown (Fig. 3C,G, 4E), and receptor mutants (Fig. Supp. 10, 12) all robustly modulate PER irrespective of the feeding status suggests that the hugin-AstA axis influences feeding behaviors both in sated and hungry flies. Additionally, their new data (Fig. Supp. 13B, C) now shows that synaptic transmission from hugin-releasing neurons is necessary for completely suppressing feeding even in sated flies. If the hugin-AstA axis engages specifically in sated (high glucose) state, disruption of this neuromodulatory system is expected to have relatively little effect in starved flies (in which the "brake" is already disengaged).

In this context, it is intriguing that the knockdown of PK2-R2 hugin receptor modestly but consistently decreases proboscis extension reflex specifically in starved flies (Fig. 3D, H). The manuscript does not discuss this interesting phenotype at all. Given the heterogeneity of hugin-releasing neurons (Fig. Supp. 7), there remains a possibility that a subset of hugin-releasing neurons and/or downstream neurons can provide a complementary (or even opposing) effect on the feeding behavior.

Given these intriguing yet unresolved issues, it is important to acknowledge that whether this system is "selectively engaged in fed states to dampen sweet sensation (in Discussion)" requires further functional investigations. Consistent effects of manipulation of the hugin-AstA system across multiple experimental approaches underscores the importance of this

molecular circuitry axis for controlling feeding behaviors. Moderation of conclusions to accommodate alternative interpretation of data will be beneficial for field to determine the precise mechanism that controls feeding behaviors in future studies.

https://doi.org/10.7554/eLife.108551.2.sa2

Reviewer #2 (Public review):

Summary:

The question of how caloric and taste information interact and consolidate remains both active and highly relevant to human health and cognition. The authors of this work sought to understand how nutrient sensing of glucose modulates sweet sensation. They found that glucose intake activates hugin signaling to AstA neurons to suppress feeding, which contributes to our mechanistic understanding of nutrient sensation. They did this by leveraging the genetic tools of Drosophila to carry out nuanced experimental manipulations, and confirmed the conservation of their main mechanism in a mammalian model. This work builds on previous studies examining sugar taste and caloric sensing, enhancing the resolution of our understanding.

Strengths:

Fully discovering neural circuits that connect body state with perception remains central to understanding homeostasis and behavior. This study expands our understanding of sugar sensing, providing mechanistic evidence for a hugin/AstA circuit that is responsive to sugar intake and suppresses feeding. In addition to effectively leveraging the genetic tools of Drosophila, this study further extends their findings into a mammalian model with the discovery that NMU neural signaling is also responsive to sugar intake.

Weaknesses:

The effect of Glut1 knockdown on PER in hugin neurons is modest in both fed and starved flies, suggesting that glucose intake through Glut1 may only be part of the mechanism. Additionally, many of the manipulations testing the "brake" circuitry throughout the study show similar effects in both fed and starved flies. This suggests that the focus of the discussion and Supplemental Figure 16 on a satiety-specific "brake" mechanism may not be fully supported by the data.

https://doi.org/10.7554/eLife.108551.2.sa1

Author response:

The following is the authors' response to the original reviews.

> ***Public Reviews:***
>
> ***Reviewer #1 (Public review):***
>
> *In this manuscript, Qin and colleagues aim to delineate a neural mechanism by which the internal satiety levels modulate the intake of sugar solution. They identified a three-step neuropeptidergic system that downregulates the sensitivity of sweet-sensing gustatory sensory neurons in sated flies. First, neurons that release a neuropeptide Hugin (which is an insect homolog of vertebrate Neuromedin U (NMU)) are in an active state when the concentration of glucose is high. This activation does not require synaptic inputs, suggesting that Hugin-releasing neurons sense hemolymph glucose levels directly. Next, the Hugin neuropeptides activate Allatostatin A (AstA)-releasing neurons via one of Hugin's receptors, PK2-R1. Finally, the released AstA neuropeptide suppresses*

> *sugar response in sugar-sensing Gr5a-expressing gustatory sensory neurons through AstA-R1 receptor. Suppression of sugar response in Gr5a-expressing neurons reduces the fly's sugar intake motivation (measured by proboscis extension reflex). They also found that NMU-expressing neurons in the ventromedial hypothalamus (VMH) of mice (which project to the rostral nucleus of the solitary tract (rNST)) are also activated by high concentrations of glucose, independent of synaptic transmission, and that injection of NMU reduces the glucose-induced activity in the downstream of NMU-expressing neurons in rNST. These data suggest that the function of Hugin neuropeptide in the fly is analogous to the function of NMU in the mouse.*
>
> *Generally, their central conclusions are well-supported by multiple independent approaches. The parallel study in mice adds a unique comparative perspective that makes the paper interesting to a wide range of readers. It is easier said than done: the rigor of this study, which effectively combined pharmacological and genetic approaches to provide multiple lines of behavioral and physiological evidence, deserves recognition and praise.*
>
> *A perceived weakness is that the behavioral effects of the manipulations of Hugin and AstA systems are modest compared to a dramatic shift of sugar solution-induced PER (the behavioral proxy of sugar sensitivity) induced by hunger, as presented in Figure 1B and E. It is true that the mutation of tyrosine hydroxylase (TH), which synthesizes dopamine, does not completely abolish the hunger-induced PER change, but the remaining effect is small. Moreover, the behavioral effect of the silencing of the Hugin/AstA system (Figure Supplement 13B, C) is difficult to interpret, leaving a possibility that this system may not be necessary for shifting PER in starved flies. These suggest that the Hugin-AstA system accounts for only a minor part of the behavioral adaptation induced by the decreased sugar levels. Their aim to "dissect out a complete neural pathway that directly senses internal energy state and modulates food-related behavioral output in the fly brain" is likely only partially achieved. While this outcome is not a shortcoming of a study per se, the depth of discussion on the mechanism of interactions between the Hugin/AstA system and the other previously characterized molecular circuit mechanisms mediating hunger-induced behavioral modulation is insufficient for readers to appreciate the novelty of this study and future challenges in the field.*

We thank the reviewer for the thoughtful comment. We agree that the behavioral effects of manipulating the Hugin–AstA system alone were considerably weaker than the pronounced PER shifts induced by starvation. We have revised our Discussion to address it by positioning our findings within the broader context of energy regulation.

More specifically, we discuss that feeding behavior is controlled by two distinct, yet synergistic, types of mechanisms:

(1) Hunger-driven 'accelerators': as the reviewer notes, pathways involving dopamine and NPF are powerful drivers of sweet sensitivity. These systems are strongly activated by hunger to promote food-seeking and consumption.

(2) Satiety-driven 'brakes': our study identifies the counterpart to those systems above, aka. a satiety-driven 'brake'. The Hugin–AstA pathway acts as a direct sensor of high internal energy (glucose), which is specifically engaged during satiety to actively suppress sweet sensation and prevent overconsumption.

This framework explains the seemingly discrepancy in effect size. The dramatic PER shift seen upon starvation is a combined result of engaging the 'accelerators' (hunger pathways like TH/NPF) while simultaneously releasing the 'brake' (our Hugin–AstA pathway being inactive).

Our manipulations, which specifically target only the 'brake' system, are therefore expected to have a more modest effect than this combined physiological state. Thus, rather than being a "minor part," the Hugin–AstA pathway is a mechanistically defined, satiety-specific circuit that is essential for the precise "braking" required for energy homeostasis. We will update our Discussion to emphasize how these 'accelerator' and 'brake' circuits must work in concert to ensure precise energy regulation.

> *In this context, authors are encouraged to confront a limitation of the study due to the lack of subtype-level circuit characterization, despite their intriguing finding that only a subtype of Hugin- and AstA-releasing neurons are responsive to the elevated level of bath-applied glucose.*

We thank the reviewer for highlighting the critical issue of subtype-level specialization within the Hugin and AstA populations.

We fully agree that the Hugin system is known for its functional heterogeneity (pleiotropy), with different Hugin neuron subclusters implicated in regulating a variety of behaviors, including feeding, aversion, and locomotion (e.g., Anna N King, Curr Biol, 2017, Andreas PLoS Biol, Sebastian et al., 2016, Nat Comm). Our finding that only a specific subcluster of Hugin neurons is responsive to glucose elevation provides a crucial first step in functionally dissecting this complexity.

we have added a dedicated paragraph to elaborate on this functional partitioning in the discussion. We propose that this subtype-level specialization allows the Hugin system to precisely link specific physiological states (like high circulating glucose) to appropriate behavioral outputs (like the suppression of sweet taste), demonstrating an elegant solution to coordinating multiple survival behaviors. Future work using high-resolution tools such as split-GAL4 and single-cell sequencing will be invaluable in fully mapping the specific functional roles corresponding to each Hugin and AstA subcluster.

> ***Reviewer #2 (Public review):***
>
> *Summary:*
>
> *The question of how caloric and taste information interact and consolidate remains both active and highly relevant to human health and cognition. The authors of this work sought to understand how nutrient sensing of glucose modulates sweet sensation. They found that glucose intake activates hugin signaling to AstA neurons to suppress feeding, which contributes to our mechanistic understanding of nutrient sensation. They did this by leveraging the genetic tools of Drosophila to carry out nuanced experimental manipulations and confirmed the conservation of their main mechanism in a mammalian model. This work builds on previous studies examining sugar taste and caloric sensing, enhancing the resolution of our understanding.*
>
> *Strengths:*
>
> *Fully discovering neural circuits that connect body state with perception remains central to understanding homeostasis and behavior. This study expands our understanding of sugar sensing, providing mechanistic evidence for a hugin/AstA circuit that is responsive to sugar intake and suppresses feeding. In addition to effectively leveraging the genetic tools of Drosophila, this study further extends their findings into a mammalian model with the discovery that NMU neural signaling is also responsive to sugar intake.*
>
> *Weaknesses:*
>
> *The effect of Glut1 knockdown on PER in hugin neurons is modest, and does not show a clear difference between fed and starved flies as might be expected if this mechanism*

> *acts as a sensor of internal energy state. This could suggest that glucose intake through Glut1 may only be part of the mechanism.*

We thank the reviewer for this insightful comment and agree that the modest behavioral effect of *Glut1* knockdown is a critical finding that warrants further clarification. This observation strongly supports the idea that internal energy state is monitored by a sophisticated and robust network, not a single, fragile component. We believe the effect size is modest for two main reasons, which we have addressed in revised Discussion.

Firstly, the effect size is likely attenuated by technical and molecular redundancy. Specifically, the RNAi-mediated knockdown of *Glut1* may be incomplete, leaving residual transporter function. Furthermore, Glut1 is likely only one part of the Hugin neuron's intrinsic sensing mechanism; other components, such as alternative glucose transporters or downstream K_{ATP} channel signaling, may provide molecular redundancy, meaning that the full energy-sensing function is not easily abolished by a single manipulation.

Secondly, and more importantly, the final feeding decision is an integrated output of competing circuits. While hunger-sensing pathways like the dopamine and NPF circuits act as powerful "accelerators" to drive sweet consumption, the Hugin–AstA pathway serves as a satiety-specific "brake." The modest effect of partially inhibiting just one component of this 'brake' system is the hallmark of a precisely regulated, multi-layered homeostatic system. We have clarified in the Discussion that the Hugin pathway represents one essential inhibitory circuit within this cooperative network that works together with the hunger-promoting systems to ensure precise control over energy intake.

> ***Reviewer #3 (Public review):***
>
> *Summary:*
>
> *This study identifies a novel energy-sensing circuit in Drosophila and mice that directly regulates sweet taste perception. In flies, hugin+ neurons function as a glucose sensor, activated through Glut1 transport and ATP-sensitive potassium channels. Once activated, hugin neurons release hugin peptide, which stimulates downstream Allatostatin A (AstA)+ neurons via PK2-R1 receptors. AstA+ neurons then inhibit sweet-sensing Gr5a+ gustatory neurons through AstA peptide and its receptor AstA-R1, reducing sweet sensitivity after feeding. Disrupting this pathway enhances sweet taste and increases food intake, while activating the pathway suppresses feeding.*
>
> *The mammalian homolog of neuromedin U (NMU) was shown to play an analogous role in mice. NMU knockout mice displayed heightened sweet preference, while NMU administration suppressed it. In addition, VMH NMU+ neurons directly sense glucose and project to rNST Calb2+ neurons, dampening sweet taste responses. The authors suggested a conserved hugin/NMU-AstA pathway that couples energy state to taste perception.*
>
> *Strengths:*
>
> *Interesting findings that extend from insects to mammals. Very comprehensive.*
>
> *Weaknesses:*
>
> *Coupling energy status to taste sensitivity is not a new story. Many pathways appear to be involved, and therefore, it raises a question as to how this hugin-AstA pathway is unique.*

The reviewer is correct that several energy-sensing pathways are known. However, we now clarify that these previously established mechanisms, such as the dopaminergic and NPF

pathways, primarily function as hunger-driven "accelerators." They are activated by low-energy states to promote sweet sensitivity and drive consumption.

The crucial, missing piece of the puzzle—which our study provides—is the satiety-specific "brake" mechanism. We identify the Hugin–AstA circuit as one of the “brakes”: a dedicated, central sensor that responds directly to high circulating glucose (satiety) to suppress sweet sensation and prevent overconsumption.

Thus, our work is unique because it defines the essential counterpart to the hunger pathways. In the revised Discussion, we have explained how these 'accelerator' (hunger) and 'brake' (satiety) systems work in concert to allow for the precise, bidirectional regulation of energy intake. Furthermore, by demonstrating that this Hugin/NMU 'brake' circuit is evolutionarily conserved in mice, our findings reveal a fundamental energy-sensing strategy and suggest that this pathway could represent a promising new therapeutic target for managing conditions of excessive food intake.

> ***Recommendations for the authors:***
>
> ***Reviewing Editor Comments:***
>
> *Considering the comments from all three reviewers, new experiments are not necessary, but the authors are welcome to provide new pieces of evidence that would strengthen their conclusions. To assist the authors with their revisions, the comments have been categorized from the highest to lowest priority based on the concerns raised by reviewers 1, 2, and 3.*
>
> *High priority:*
>
> *(1) Acknowledgement of partial phenotypes by the genetic manipulations, especially relative to other neuromodulators that are involved in the adjustment of sugar sensitivity after starvation (1, 2).*

Please see our responses to the Public Review 1 for details.

> *(2) Detailed discussion on the novelty of the present work, also in light of previous studies both in flies and mammals (known Drosophila modulators, as well as NMU-rNST circuit on sugar sensation) (1, 2, 3).*

Please see our responses to the Public Review 3 for details.

> *(3) Medium priority:*
>
> *• Discussions on the subtype-specific function of hugin neurons (1).*

Please see our responses to the Public Review 1 for details.

> *• Discussions on the pleiotropic effect of changes in the level of circulating sugar (including release of other sugar types) (2, 3).*

We agree that circulating sugars represent a complex, systemic signal with broad, pleiotropic effects, and we have expanded our Discussion to address this.

We will discuss the functional distinction between key hemolymph sugars, such as trehalose (the main circulating sugar, critical for stress/flight) and glucose (the primary, rapidly mobilized energy currency). While various sugars collectively influence metabolic status, our study’s unique focus is on the direct neural link between internal energy and sweet taste modulation. We clarify that our work precisely identifies glucose as the direct, key ligand for the Hugin satiety circuit, thus providing a concrete, mechanistically defined link from systemic energy complexity to the specific regulation of sweet sensation.

> • *Illustration or clear explanations of sugar application methods in mouse experiments (ex. Figure 5F vs Figure 5M), as well as discussion on the concentration of sugar solutions used (3).*

We have added the relevant details in the figure legends and explain the rationale for using this concentration of sugar in the results.

> • *Less saturated image for Figure 5K (3).*

We have adjusted Figure 5K to reduce image saturation for clarity.

> • *Discussions on the modest effect of NMU on rNST neurons (Figure 5M) (3).*

In the revised results, we have discussed that the modest suppression of rNST activity likely reflects partial peptide diffusion and the heterogeneous composition of sweet-responsive rNST neurons.

> *(4) Low priority:*
>
> • *Systematic quantification of multiple types of sugars after starvation (3).*

We agree that circulating sugars represent a complex metabolic milieu, and a fully systematic biochemical quantification of individual hemolymph sugars after starvation would be informative. While such analyses are beyond the scope of the present study, we have addressed this point at the functional level by systematically pre-feeding flies with different types of dietary sugars prior to PER assays.

We find that multiple sugars are capable of suppressing PER, indicating that satiety-related behavioral inhibition is not unique to a single carbohydrate source. Notably, sucrose produces the strongest suppression, consistent with its rapid metabolic conversion and effectiveness in elevating internal glucose levels. These results support the notion that diverse dietary sugars converge on a common satiety-signaling mechanism, while our mechanistic analyses specifically identify glucose as the key ligand engaging the Hugin satiety circuit.

We now clarify this distinction in the revised Discussion.

> • *Testing Gr64f neurons or mutants (3).*

Our results indicate that energy sensing in the CNS suppresses sweet-sensing neuron activity (e.g., via hyperpolarization) rather than directly blocking sugar binding to receptors. Thus, sweet perception—not sugar detection—is inhibited. As evidence, in Figure supplementary4 we measured the PER to fructose and trehalose. Although Gr5a and Gr64a differ in their sensitivity to these sugars, the CNS energy state consistently suppresses sweet perception for both. As Reviewer 3 noted, Gr5a and Gr64f are co-expressed in sweet neurons; while they respond to different sugars, their labeling of the neurons is largely equivalent.

> • *Testing sugar preference (glucose vs. other sugars) (3)*

Since our primary goal was to identify a direct satiety-sensing and sensory-modulating circuit —the "brake" mechanism—PER served as the most suitable and mechanistically specific readout. While manipulation of the Hugin–AstA circuit influences internal state, and therefore likely alters long-term sugar preference, investigating the integration of this pathway with reward and post-ingestive signaling is a critical question that lies beyond the scope of the current study.

> • *Cell type-specific knockout of NMU (3).*

Achieving a cell type-specific knockout of NMU using the Cre approach is not feasible in the short term. While previous studies have reported the role of NMU in the VMH region in regulating feeding, our contribution lies in revealing how these neurons sense energy. We also show that these neurons project to the vicinity of Calb2 neurons and that the neuropeptide can suppress Calb2 neuronal activity. This essentially demonstrates that the hugin–Gr5a pathway in *Drosophila* is conserved in mice. We believe that a detailed dissection of the precise circuitry in mice is more appropriate to address in a subsequent study.

> • *Explanation of NMU detection in Figure 5K (3): this is GFP expressed by the Cre-dependent virus.*

We have revised the Figure 5K legend to clarify that NMU^+ neurons are labeled by GFP expression from a Cre-dependent AAV2/1-DIO-GFP, which undergoes anterograde trans-synaptic transfer. We further explain that GFP expression in rNST neurons requires local AAV-Cre injection, enabling identification of postsynaptic $Calb2^+$ target neurons.

> • *Neuronal manipulation of NMU neurons by optogenetics or DREADD.*

Please see our responses to the question "Cell type-specific knockout of NMU."

> ***Reviewer #1 (Recommendations for the authors):***
>
> *A major concern about the study is that the effect of genetic manipulations on Hugin/AstA system appears to account for only a small part of the dramatic shift of PER probability toward smaller concentrations of sucrose solutions among starved flies. In Figure 1B and E, PER probability is significantly higher among starved flies in response to 10-200mM of sucrose solutions than fed flies. Compared to this, RNAi knockdown of glucose transporter in hugin neurons (Figure 2C), PK2-R1 pan-neuronally (Figure 3C) or in AstA-releasing neurons (Figure 3G), AstA-R1 in Gr5a neurons (Figure 4E), systemic mutation of PK-R2 (Figure Supplement 10) and AstA-R1 (Figure Supplement 12) all produce relatively minor behavioral changes. Consistent with previous works, the mutation of TH causes a robust decrease of PER across the entire range of sucrose concentration tested (Figure Supplement 1).*
>
> *These discrepancies can be caused by many technical limitations that cannot be readily addressed. For instance, the large effect of TH can be confounded by the pleiotropic behavioral effect of the lack of dopamine. RNAi can suffer from incomplete elimination of targeted genes. However, the relatively small behavioral effect size of these manipulations cannot be entirely ignored in light of previous publications, which point to the importance of other neuromodulators such as dopamine, serotonin, Akh, and NPF, on sugar sensitivity (Marella et al., 2012; Inagaki et al., 2014; Yao et al., 2022), as well as other potentially parallel glucose-sensing systems, including Gr43a-expressing cells (Miyamoto et al., 2012) and sNPF-expressing CN neurons (Oh et al., 2019). While the neuropeptides initially tested (Figure 1) are not poor choices, it is a missed opportunity that so many other neuromodulators were excluded from the initial search.*

We appreciate the reviewer's detailed analysis and agree that the magnitude of behavioral effects produced by manipulating the hugin–AstA pathway is smaller than the dramatic shift in PER observed under starvation conditions. This comparison is important and highlights a central conceptual point of our study.

Starvation represents a compound physiological state that simultaneously engages multiple hunger-promoting neuromodulatory systems—most prominently dopaminergic and NPF pathways—while also releasing satiety-associated inhibitory signals. As shown previously and confirmed here (Figure supplementary 1), manipulation of dopamine synthesis produces

a broad and robust reduction in PER across sucrose concentrations, consistent with its role as a powerful hunger-driven modulator.

By contrast, our genetic manipulations specifically target a satiety-associated inhibitory circuit—the hugin–AstA pathway—that is selectively engaged by high internal glucose levels. Manipulating this pathway alone therefore isolates a single “brake” component of feeding regulation, rather than recapitulating the full physiological state of starvation, which combines both accelerator activation and brake release. Accordingly, the more modest behavioral effects we observe are an expected consequence of dissecting one defined regulatory module from a larger, cooperative network.

We agree that multiple neuromodulators, including dopamine, serotonin, Akh, NPF, and others, as well as parallel glucose-sensing systems such as Gr43a-expressing cells and sNPF-expressing CN neurons, contribute to the regulation of sugar sensitivity. Rather than aiming to exhaustively screen all neuromodulators, our study was designed to identify and mechanistically define a central, glucose-responsive satiety sensor that directly links internal energy state to sweet taste modulation. In the revised discussion, we now explicitly position the hugin–AstA circuit as one essential, satiety-specific component within this broader regulatory landscape and discuss how it functionally complements previously characterized hunger-driven pathways.

> *I am also confused by the results of Shibirets1-mediated silencing of Hugin and AstA neurons (Figure Supplement 13B, C). It is unclear to me why a feeding assay was used instead of PER, like the activation experiments. Feeding (ingestion) and PER are qualitatively different types of behavior, which cannot be directly compared. Moreover, the definition of "fold change" is not provided either in the figure legend or in the Materials and Methods section, making it difficult to understand what the figure means.*

We thank the reviewer for pointing out this important issue regarding the interpretation of the Shibire^ts1-mediated silencing experiments. We agree that proboscis extension reflex (PER) and feeding/ingestion assays reflect qualitatively different behavioral processes and should not be directly compared.

In the original submission, feeding assays were used to assess the effect of neuronal silencing, which led to ambiguity when comparing these results with PER-based activation experiments. To directly address this concern and ensure consistency across behavioral readouts, we have now performed additional PER experiments under the same Shibire^ts1-mediated silencing conditions.

These new data demonstrate that acute silencing of hugin neurons significantly enhances PER responses to sucrose (Figure supplementary 13B), indicating increased sweet sensitivity. This result is fully consistent with our activation experiments and supports the conclusion that the hugin–AstA pathway suppresses sweet taste perception under satiety conditions.

In addition, we have revised the figure legend to explicitly define the “fold change” metric used in the behavioral analysis, clarifying how the values were calculated and normalized. Together, these changes resolve the ambiguity raised by the reviewer and strengthen the behavioral consistency of our conclusions.

> *Of note, Marella et al. (2012) reported that silencing of Hugin-releasing neurons did not affect PER. It is therefore possible that the Hugin system is sufficient, but not necessary, for modulating PER under food deprivation.*

We agree that their observation—that silencing Hugin-releasing neurons does not alter PER in starved flies—is consistent with a state-dependent role of the Hugin system in feeding regulation.

In starved animals, dopaminergic TH^+ neurons are strongly activated and promote high PER responsiveness, while circulating glucose levels are low, placing Hugin neurons in a relatively inactive state. Under such conditions, further silencing of Hugin neurons would be expected to produce minimal additional effects on PER, which likely explains the results reported by Marella et al.

Importantly, our data show that preventing the starvation-associated reduction in Hugin neuronal activity—by thermogenetic activation of $Hugin^+$ neurons (Hugin–TrpA1; Figure 1D)—significantly suppresses the hunger-induced enhancement of PER. These results indicate that dynamic downregulation of Hugin neuronal activity is a critical component of the normal behavioral shift in sweet sensitivity in response to food deprivation. Thus, while Hugin neurons may not be required to further modulate PER once animals are already in a strongly starved state, their regulated activity change is essential for mediating state-dependent modulation of sweet taste behavior. We have added discussion in the revised manuscript.

> *While no new experiments are requested, it is important for authors to acknowledge the limited effect size of Hugin/AstA manipulation. In the current manuscript, the authors briefly mention the previous works (lines 460-462, 472-474), which is insufficient. Discussions must include how the Hugin/AstA system may "complement these established mechanisms (line 460)" (described in the references listed above), under what situations this novel Hugin/AstA system can be relevant for controlling PER, and why the fly is equipped with seemingly redundant systems for sensing internal glucose levels and controlling feeding behavior. Without these discussions, it is difficult to recognize the novelty of the presented work. The data appears largely to be a minor and incremental progress on an already mature field.*

In the revised manuscript, we have substantially expanded the Discussion to explicitly acknowledge this limited effect size and to clarify the functional role of the Hugin–AstA pathway within the broader energy-regulatory network. We now emphasize that this circuit represents a satiety-specific inhibitory branch that complements, rather than replaces, previously described hunger-promoting systems such as dopaminergic, NPF, and AKH circuits.

Importantly, we discuss the specific physiological conditions under which the Hugin–AstA system is most relevant—namely, post-feeding and high-glucose states. Unlike hunger circuits that amplify sweet sensitivity during starvation, the Hugin–AstA pathway directly senses circulating glucose and rapidly suppresses sweet taste perception when energy is sufficient, thereby acting as a brake to prevent overconsumption.

We further address the apparent redundancy among internal sugar-sensing systems. Rather than being redundant, these pathways form a coordinated and layered network with distinct sugar specificities, temporal dynamics, and functional roles. For example, $Gr43a^+$ neurons primarily detect fructose, whereas hemolymph glucose represents the principal energetic currency in *Drosophila*. The use of multiple internal sugar sensors allows flies to fine-tune feeding decisions across different nutritional contexts and timescales.

Finally, we expand the Discussion to highlight that although the Hugin–AstA circuit constitutes only one branch of the energy-sensing network, its disruption leads to excessive energy intake (Figure supplementary 13C-E, G) and increased fat accumulation (Figure S13F), underscoring its physiological relevance. We also discuss how this pathway likely interacts with other neuromodulatory systems, including TH^+ dopaminergic and NPF^+ neurons, to collectively orchestrate adaptive feeding behavior and energy homeostasis.

Together, these additions clarify that our work does not simply add another neuromodulator

to an already mature field, but instead identifies a distinct glucose-sensing, satiety-linked mechanism that fills a conceptual gap between internal energy state detection and sensory modulation.

> *Another perceived weakness is the lack of subtype-level dissection among Hugin- and AstA-releasing neurons. I make a justified request to narrow down the behaviorally relevant neuron to one (or one type), which is based on a widespread but unreasonable and dangerous assumption that every behavior must be controlled by one neuron. However, the authors present very interesting data that only a subset of Hugin- and AstA-releasing neurons responds to higher levels of sucrose (Figure 1H, Figure Supplement 7A, B), which leads to a hypothesis that a specific subtype within each peptidergic neuronal group is responsible for starvation-induced behavioral change. The authors only briefly touch upon this (lines 217-218), but this is an important hypothesis that requires further discussion.*

We thank the reviewer for highlighting the importance of neuronal heterogeneity within the Hugin- and AstA-releasing populations. We fully agree that the observation that only a subset of $Hugin^+$ and $AstA^+$ neurons responds to elevated sucrose levels (Figure 1H; Figure Supplement 7A, B) strongly suggests functional specialization within these peptidergic groups.

In the revised Discussion, we now explicitly propose that distinct subtypes of Hugin and AstA neurons differentially contribute to energy sensing and feeding modulation. We suggest that glucose-responsive subpopulations may be specifically engaged in satiety signaling, whereas other neurons within the same genetic classes may participate in additional physiological or behavioral processes. This heterogeneity provides a plausible explanation for the partial behavioral effects observed following population-level manipulations. Although we did not perform subtype-specific perturbations in this study, our findings provide a foundation for identifying these subtypes in future work using split-GAL4 lines and connectomic datasets.

> *These issues are more important than the sprawling and unfocused review of various hunger and satiety-controlling systems across species in the Introduction. Lines 53-108 contain only tangential information to the main conclusion of the paper. Both the Introduction and Discussion sections must be completely restructured so that readers understand what is already known about hunger-induced changes in feeding-related behavior, what is a missing gap of knowledge in neural mechanisms controlling behavioral adaptation under starvation, and why Hugin/NMU is an interesting target in this context.*

We thank the reviewer for this important structural critique. We agree that, in the original manuscript, the Introduction placed disproportionate emphasis on a broad survey of hunger- and satiety-regulating systems across species, which may have obscured the central conceptual advance of this study.

In the revised manuscript, we have substantially restructured both the Introduction and the Discussion to sharpen the narrative focus and clarify the specific knowledge gap addressed by our work.

First, the Introduction has been streamlined to focus on what is already known about hunger-induced modulation of feeding-related behaviors, particularly sweet taste sensitivity and PER in *Drosophila*. We now emphasize that prior studies have predominantly characterized hunger-activated, feeding-promoting pathways (e.g., dopaminergic, NPF, AKH systems) that act as accelerators of food-seeking behavior.

Second, we explicitly define the missing gap in knowledge: while hunger-driven mechanisms are well studied, it remains unclear how satiety states—specifically elevated internal glucose

levels—are directly sensed by central neurons and translated into suppression of sensory gain and feeding behavior.

Third, we reposition Hugin/NMU as an attractive and conceptually distinct target because of its peptidergic nature, evolutionary conservation, and previously reported but mechanistically unresolved links to feeding regulation. This framing motivates our central question: whether Hugin/NMU neurons function as a direct internal energy sensor that actively implements a satiety-specific inhibitory control over taste perception.

In parallel, the Discussion has been reorganized to avoid an unfocused review of feeding circuits across species and instead to interpret our findings within a clear conceptual framework. We now emphasize that the Hugin–AstA (and NMU) pathway represents a satiety-driven “brake” that complements, rather than duplicates, established hunger-driven “accelerator” circuits. This restructuring clarifies both the novelty of our findings and their relevance within the existing literature.

> ***Reviewer #2 (Recommendations for the authors):***
>
> *When discussing the results of Figure 1, such as lines 203-204, "These results demonstrate that sugar intake inhibits sweet sensation, probably via increasing circulating sugar levels" it may be worth discussing the known impact of sweet sensation experience on future sweet taste responses. With the data shown here, it is difficult to conclusively separate blood glucose levels from the sweet sensation that happens during the re-feeding. The "normal diet minus sucrose" does not blunt the starved PER effect, but that could potentially be impacted by either/both sugar intake or sweet taste.*

We thank the reviewer for this thoughtful and important point. We agree that sweet taste experience itself can influence subsequent sweet sensitivity, and that separating the contribution of sensory experience from nutrient-derived internal energy is non-trivial.

In the revised manuscript, we have clarified the experimental timing by explicitly stating that PER was assessed 15 minutes after refeeding. At this time point, hemolymph glucose levels have returned to baseline (Figure supplementary 5), supporting the physiological relevance of glucose-dependent activation of Hugin neurons under our experimental conditions.

We also acknowledge that sweet taste exposure can induce sensory adaptation and modulate future taste responses. To directly address this potential confound, we performed additional control experiments during revision (Figure supplementary 4B) in which starved flies were refed with sorbitol (caloric but not sweet) or arabinose (sweet but non-nutritive). We found that both manipulations partially reduced PER, but neither recapitulated the full suppressive effect of sucrose refeeding.

These results indicate that sweet taste experience and metabolic energy contribute in parallel to the regulation of sweet sensitivity. Importantly, the incomplete effects of sorbitol or arabinose alone suggest that neither sensory adaptation nor caloric value is sufficient by itself to fully account for the observed PER suppression.

Accordingly, we have revised the Discussion to clarify that the Hugin–AstA pathway likely operates within a broader, multi-layered regulatory framework, integrating internal metabolic state with sensory experience, rather than acting as a sole determinant of post-feeding sweet sensitivity. This clarification avoids over-attribution of the behavioral effect to circulating glucose alone while preserving the central conclusion that internal energy state is a key modulator of sweet perception.

> *Blocking cellular sugar intake or metabolism could be impacting the ability of neurons to function, distinct from any specific intracellular regulatory mechanism that glucose or its*

> *derivatives might be involved with. That may be a caveat worth mentioning in the results or discussion.*

We thank the reviewer for raising this important caveat. We agree that blocking cellular sugar uptake or metabolism could, in principle, impair neuronal function in a nonspecific manner, independent of any dedicated intracellular glucose-sensing mechanism.

In the revised manuscript, we now explicitly acknowledge this possibility and clarify the scope of our interpretation. Several features of our data argue against a generalized loss of neuronal function as the primary explanation. First, the behavioral and physiological effects observed upon manipulation of glucose transport or K_{ATP} channel activity are rapid and reversible, consistent with state-dependent modulation rather than chronic metabolic failure. Second, these manipulations selectively affect sweet sensitivity and feeding-related behaviors, without causing gross deficits in proboscis extension or neuronal responsiveness.

Accordingly, we have revised the Results to emphasize that while intracellular glucose metabolism is required for normal neuronal activity, our findings specifically support a role for glucose-dependent modulation of neuronal excitability in satiety signaling, rather than a nonspecific energetic impairment.

> *Minor suggestions:*
>
> *(1) Figure 2G: "Pryuvate" -> "Pyruvate."*

We have corrected “Pryuvate” to “Pyruvate”

> *(2) "Fly" methods section: it says that flies were kept on 2% agar for 12 hours for starvation, but in the Figure 1A description, it says 24 hours.*

We have corrected the description in Figure 1A.

> ***Reviewer #3 (Recommendations for the authors):***
>
> *(1) SEZ Hugin+ and AstA+ neurons were activated by glucose (Figures 1G, 1I), yet hemolymph also contains trehalose and fructose. For instance, DH44 neurons respond broadly to all hemolymph sugars (Dus et al., 2015), while Gr43a neurons specifically detect fructose (Miyamoto et al., 2012). The present study does not clarify whether Hugin+ or AstA+ neurons are similarly sugar-specific or more broadly tuned. A systematic analysis is needed to determine whether these circuits are selective for glucose.*

We thank the reviewer for raising this important question regarding sugar specificity. We agree that hemolymph contains multiple sugars, including trehalose and fructose, and that distinct neural systems have been shown to differ in their tuning breadth. To address this issue, we performed additional experiments during revision in which starved wild-type flies were refed with different sugars—including sucrose, fructose, trehalose, and sorbitol—followed by PER measurements. We found that sucrose refeeding produced the strongest suppression of PER, whereas fructose, trehalose, and sorbitol induced weaker effects (Figuresupplementary 4A).

We interpret these results as suggesting a preferential sensitivity of the Hugin/AstA pathway to glucose availability rather than a broad responsiveness to all circulating sugars. One plausible explanation is that fructose, trehalose, and sorbitol require peripheral metabolic conversion before contributing to intracellular glucose levels in neurons, whereas sucrose feeding rapidly restores hemolymph glucose within the 15-minute time window used in our experiments (Figure supplementary 5).

Importantly, we now clarify in the revised Results and Discussion that our data support a functional preference for glucose under physiological conditions, rather than excluding the

possibility that other sugars may influence this circuit indirectly or on longer timescales.

> *(2) The authors state that SEZ, but not VNC, Hugin+ neurons regulate AstA activity (lines 318-319). However, comparison of Figure Supplement 8B with the severing sample in Figure Supplement 11B shows a more pronounced reduction of sweet sensation under hug>TrpA1 activation. Although the absolute response in Figure 3F (in vivo) is higher than that in the cut-off preparation (Figure S11), comparison of Figure S11C with Figure 3F indicates that hug+ neurons drive an AstA+ calcium transient more than fourfold greater in the presence of VNC neurons. Thus, the contribution of Hugin+ VNC neurons cannot be dismissed, and the conclusion should be revised accordingly.*

We thank the reviewer for this careful and quantitative comparison. We agree that our original wording overstated the exclusivity of SEZ Hugin$^+$ neurons in regulating AstA activity.

Upon closer examination of the data, we now acknowledge that VNC Hugin$^+$ neurons likely contribute to AstA activation. As the reviewer points out, the AstA$^+$ calcium response evoked by Hugin activation is substantially larger when VNC neurons are intact (Figure supplementary11C) compared with the cut preparation (Figure 3F), indicating that descending inputs from the VNC can potentiate AstA neuronal activity.

Accordingly, we have revised the manuscript to state that SEZ Hugin$^+$ neurons play a predominant role in driving AstA responses relevant to sweet sensation, while VNC Hugin$^+$ neurons provide additional modulatory input that enhances the overall magnitude of Hugin signaling. These revisions have been made in the Results to more accurately reflect the contributions of distinct Hugin subpopulations.

> *(3) In Figure 4D, you show AstA-R1 co-localized with Gr5a-expressing cells. However, Gr5a-expressing cells also co-express Gr64f in labellum (Fuji et al., 2015, Current Biology). Are the authors sure that the sweet sensation they described is Gr5a-specific? Testing Gr64f is essential. Moreover, Fuji et al. demonstrated that Gr5a loss-of-function mutation impairs not only sucrose but also maltose, fructose, and trehalose sensation. This raises a question of whether the Hug+ and AstA+ neurons identified in the current study contribute to sensing sugars beyond sucrose. Additional experiments are required to clarify this point.*

Please see our responses to the Reviewing Editor Comments (4).

> *(4) While nutritive sugar sensors such as Dh44 neurons have been directly implicated in sugar preference (Dus et al., 2015, Neuron), this study examines the hug+,AstA+, Gr5a neuronal circuit only in the context of PER responses. Why is sugar preference not assessed here, especially given that in mice, the comparison was made using preference tests?*

We thank the reviewer for this insightful question. We agree that sugar preference assays provide important information about feeding decisions and reward-based behavior. In the present study, however, we deliberately focused on the proboscis extension reflex (PER) because it offers a direct, quantitative, and temporally precise readout of sweet sensory sensitivity at the sensory–motor level.

PER allows us to isolate changes in taste perception itself, largely independent of post-ingestive reinforcement, learning, or motivational state, all of which strongly influence preference-based assays. This distinction is particularly important given our central goal of identifying a circuit that directly links internal energy sensing to modulation of peripheral sweet-sensing neurons.

By contrast, sugar preference reflects an integrated behavioral outcome combining sensory input, internal state, and post-ingestive reward signals, including those mediated by DH44

neurons and other nutritive sensing pathways. We therefore chose PER as the most mechanistically specific assay to dissect the Hugin–AstA–Gr5a pathway. We now explicitly acknowledge in the revised Discussion that determining how this satiety-linked sensory modulation interacts with reward and post-ingestive circuits to shape long-term sugar preference will be an important direction for future studies.

> *Several other concerns:*
>
> *(5) The intraperitoneal injection of NMU is interpreted as reflecting a brain-specific NMU effect, but such systemic delivery cannot exclude peripheral actions. In Figure 5D, the use of whole-body KO mice is insufficient; targeted manipulations (e.g., NMU-Cre-driven inactivation) are required to establish circuit-specific behavioral roles.*

Please see our responses to the Reviewing Editor Comments (Low priority)

> *(6) In Figure 5F and 5M, neural activity is measured under different conditions: gastric glucose infusion in 5F versus glucose licking in 5M. To establish that NMU VMH neurons and Calb2 rNST neurons belong to the same circuit, this discrepancy in stimulation timing must be resolved to support the conclusions.*

We thank the reviewer for pointing out this important issue regarding stimulation paradigms in Figures 5F and 5M. We agree that the difference between gastric glucose infusion and glucose licking requires explicit clarification.

In the revised manuscript, we now clearly state that these two paradigms were intentionally designed to probe complementary levels of the same NMU–Calb2 circuit. In Figure 5F, gastric glucose infusion was used to isolate the internal energy-sensing property of VMH NMU^+ neurons, independent of oral sensory input, motor behavior, or reward expectation. This experiment establishes that NMU^+ neurons are directly activated by elevated circulating glucose.

By contrast, Figures 5M examined how activation of this NMU pathway modulates downstream $Calb2^+$ rNST neurons under physiologically relevant feeding conditions, in which sweet taste signals are naturally evoked by licking. This design allows us to test the functional consequence of NMU signaling on sweet-responsive rNST neurons during normal sensory processing.

Although the route and timing of glucose delivery differ, both paradigms converge on a unified circuit model: internal glucose elevation activates VMH NMU^+ neurons, and NMU signaling suppresses sweet-driven activity in $Calb2^+$ rNST neurons. We have revised the Results and figure legends to explicitly describe this layered experimental logic and to clarify that Figures 5F and 5M together establish distinct but connected nodes of the same circuit.

> *(7) Figure 5I-J. The glucose concentration used appears excessively high. In mammals, blood glucose in the sated state is ~7-8 mM. It is unclear whether the observed responses represent physiological effects or artifacts of supraphysiological stimulation. Additional experiments with lower glucose concentrations would strengthen the study.*

We thank the reviewer for raising this important concern regarding the glucose concentration used in Figure 5I–J. We agree that the concentration applied in ex vivo slice experiments exceeds the typical physiological range of circulating glucose.

This higher concentration was intentionally chosen to ensure reliable neuronal activation in acute brain slices, where glucose diffusion, uptake, and metabolic access are substantially slower than in vivo. Similar approaches have been widely used in studies of glucose-sensitive hypothalamic neurons to overcome these technical limitations (e.g., Kim et al., 2025., Neuron).

Importantly, the physiological relevance of our findings is supported by in vivo fiber photometry experiments, which demonstrate that VMH NMU$^+$ neurons are robustly activated following normal sugar ingestion under physiological conditions. Thus, while supraphysiological glucose was used to establish glucose responsiveness ex vivo, our in vivo data confirm that NMU$^+$ neurons respond to glucose elevations within the normal physiological range.

> *(8) Figure 5K. The VMH images are inconsistently oriented compared with Figure 5E, lacking a 3v landmark. The NMU detection method (IHC or FISH) is not specified in the legend. The GFP-Calb2 signal is heavily saturated, making it difficult to distinguish true signals from artifacts. These issues undermine interpretability.*

We thank the reviewer for pointing out these issues. In the revised manuscript, VMH images in Figure 5K have been reoriented to match Figure 5E, and the third ventricle (3v) is now indicated as an anatomical landmark. The figure legend has been revised to clarify that NMU$^+$ neurons are identified by GFP expression from a Cre-dependent AAV2/1-DIO-GFP injected into NMU-Cre mice, rather than by NMU immunohistochemistry or FISH. In addition, GFP–Calb2 images have been reprocessed to clearly distinguish true signals from background and imaging artifacts.

> *(9) Figure 5L-M. Details of the NMU injection method are absent (route, dose, delivery parameters). The number of animals (n) is also not reported. Furthermore, AUC reduction alone is not sufficient evidence of robust inhibition. To convincingly demonstrate causality, NMU-IRES-Cre mice should be combined with DREADD or optogenetic approaches to directly inhibit NMU neurons and test whether rNST Calb2 activity is reduced.*

We thank the reviewer for these helpful comments. We have revised the manuscript to include all missing methodological details. These details are now clearly described in the Methods section and figure legend.

We fully acknowledge that cell-type–specific manipulations, such as DREADD or optogenetic inhibition of NMU neurons, would provide more definitive causal evidence. However, our main goal in the mouse experiments was to demonstrate that NMU$^+$ neurons can directly sense glucose and modulate sweet sensitivity, thereby supporting the evolutionary conservation of the Hugin mechanism identified in *Drosophila*. Detailed dissection of the downstream circuit architecture and behavioral consequences in mammals is indeed an important direction for future research, but it lies beyond the current study's primary focus on cross-species conservation.

> *(10) In Drosophila, hugin neurons respond selectively to nutritive glucose (Fig. 2H), but whether NMU neurons share this property is unknown. Notably, Calb2 neurons in the rNST respond to the artificial sweetener AceK (Hao Jin et al., 2021, Cell), leaving open whether the NMU-rNST circuit is calorie-dependent or calorie-independent.*

We have added a statement in the Discussion acknowledging this limitation and emphasizing that future work will be needed to test whether the NMU–Calb2 circuit is selectively engaged by metabolically active sugars or also by sweet taste signals independent of caloric value.

> *Minor comments*
>
> *(11) All bar graphs should include individual data points.*

We have added individual data points to all bar graphs.

> *(12) In Figures 3E, 4C, and 4D, it appears that a combination of GAL4 and LexA was used, but the information about the fly lines is missing.*

We have now included the complete list of fly lines used for these experiments, including their genotypes and sources.

> *(13) The source for PK2-R1 KO, AstA-R1 KO fly lines and NMU-IRES-Cre, Calb2-IRES-Cre mice is missing.*

We have added the complete source information for all genetic lines mentioned.

> *(14) Figure 5B-D, This is a sucrose preference test, so why is the y-axis labeled as glucose? Is this an error, or were the values converted to glucose equivalents?*

We thank the reviewer for catching this mistake. The assay shown in Figure 5B–D measured sucrose preference, not glucose preference. The inconsistency resulted from a typographical error in the Methods description. In the revised manuscript, we have corrected this error to clearly state that sucrose was used in the preference test,

> *(15) Supplementary Figure 15. The NMU images are of poor quality and should be improved.*

The punctate appearance of NMU signals in Supplementary Figure 15 is not due to poor image quality but rather reflects the physiological distribution of the NMU neuropeptide. As NMU is stored in secretory vesicles within neuronal terminals and somata, its immunostaining typically appears as discrete puncta rather than diffuse cytoplasmic labeling.

> ***Editor's note:***
>
> *Should you choose to revise your manuscript, if you have not already done so, please include full statistical reporting including exact p-values wherever possible alongside the summary statistics (test statistic and df) and, where appropriate, 95% confidence intervals. These should be reported for all key questions and not only when the p-value is less than 0.05 in the main manuscript.*
>
> *Readers would also benefit from noting that the mice were male and discussion of the exclusion of females.*

In the revised manuscript, we have included full statistical reporting for all key experiments in the resource data. Regarding animal sex, we confirm that all mouse experiments were conducted using male mice. This choice was made to minimize variability caused by hormonal cycles in females, which can influence feeding behavior and glucose metabolism. We have now explicitly stated this information in the Methods section and included a brief discussion noting that sex-specific differences in NMU–Calb2 circuitry and feeding regulation represent an important question for future investigation.

https://doi.org/10.7554/eLife.108551.2.sa0